(4)

AeroChem TP-489

Production and Coating of Pure Boron Powders

Hartwell F. Calcote
Robert J. Gill
Charles H. Berman
William Felder

AeroChem Research Laboratories, Inc.
Princeton, New Jersey 08542

March 1990

Contract N00014-89-C-0246

Prepared for

Office of Naval Research
Arlington, Virginia 22217-5000

UNCLASSIFIED
SECURITY CLASSIFICATION OF THIS PAGE

REPORT DOCUMENTATION PAGE

Form Approved
OMB No. 0704-0188

1a. REPORT SECURITY CLASSIFICATION Unclassified	1b. RESTRICTIVE MARKINGS
2a. SECURITY CLASSIFICATION AUTHORITY	3. DISTRIBUTION/AVAILABILITY OF REPORT
2b. DECLASSIFICATION/DOWNGRADING SCHEDULE	
4. PERFORMING ORGANIZATION REPORT NUMBER(S) AeroChem TP-489	5. MONITORING ORGANIZATION REPORT NUMBER(S)
6a. NAME OF PERFORMING ORGANIZATION AeroChem Research Laboratories, Inc.	6b. OFFICE SYMBOL (*If applicable*) / 7a. NAME OF MONITORING ORGANIZATION
6c. ADDRESS (*City, State, and ZIP Code*) P.O. Box 12 Princeton, New Jersey 08542	7b. ADDRESS (*City, State, and ZIP Code*)
8a. NAME OF FUNDING/SPONSORING ORGANIZATION Office of Naval Research	8b. OFFICE SYMBOL (*If applicable*) / 9. PROCUREMENT INSTRUMENT IDENTIFICATION NUMBER N00014-89-0246
8c. ADDRESS (*City, State, and ZIP Code*) 800 N. Quincy St. Arlington, Virginia 22217-5000	10. SOURCE OF FUNDING NUMBERS

PROGRAM ELEMENT NO.	PROJECT NO.	TASK NO.	WORK UNIT ACCESSION NO.

11. TITLE (*Include Security Classification*)
Production and Coating of Pure Boron Powders

12. PERSONAL AUTHOR(S)
Calcote, Hartwell F., Gill, Robert J., Berman, Charles H., and Felder, William

13a. TYPE OF REPORT	13b. TIME COVERED	14. DATE OF REPORT (*Year, Month, Day*)	15. PAGE COUNT
Final	FROM 89-9-1 TO 90-2-28	1990, March 30	58

16. SUPPLEMENTARY NOTATION

17. COSATI CODES			18. SUBJECT TERMS (*Continue on reverse if necessary and identify by block number*)
FIELD	GROUP	SUB-GROUP	Boron Fuel; Combustion Synthesis; Particles; Coated Particles; Particle Separation

19. ABSTRACT (*Continue on reverse if necessary and identify by block number*)

Boron is an attractive fuel because of its potential energy release with oxygen and because of its light weight. It is, however, difficult to incorporate into a fuel system because an oxide layer forms on the surface and suppresses combustion. A new synthesis process has been evaluated for the preparation of boron fuel particles coated with titanium. The titanium coating prevents oxide from forming and aids in the combustion, Pure boron particles are produced by reaction of sodium with boron trichloride, the products expanded through a supersonic nozzle, in which titanium tetrachloride is added to produce titanium. The titanium coats the boron particle. The coated particles are separated from the gaseous sodium chloride by a new type supersonic virtual impact collector. The process has been analyzed by computer modeling and an apparatus has been designed to test the concept and prepare coated boron fuel particles for evaluation.

20. DISTRIBUTION/AVAILABILITY OF ABSTRACT	21. ABSTRACT SECURITY CLASSIFICATION
☒ UNCLASSIFIED/UNLIMITED ☐ SAME AS RPT. ☐ DTIC USERS	Unclassified

22a. NAME OF RESPONSIBLE INDIVIDUAL	22b. TELEPHONE (*Include Area Code*)	22c. OFFICE SYMBOL
Dr. Gabriel Roy	202-696-4406	Code 1132P

DD Form 1473, JUN 86 *Previous editions are obsolete.* SECURITY CLASSIFICATION OF THIS PAGE
UNCLASSIFIED

CONTENTS

FIGURES

TABLES

SYMBOLS, ABBREVIATIONS, AND ACRONYMS

A	=	particle surface area
A_f	=	filter surface area
C_1	=	concentration of NaCl behind the virtual impact collector aperture
C_2	=	concentration of NaCl behind the shock and in front of the virtual impact collector aperture
C_D	=	drag coefficient
D	=	diffusion coefficient
D_p	=	particle diameter
F	=	flux of NaCl across the aperture of the virtual impact collector aperture
$H(a,b,c)$	=	enthalpy of substance "a" in "b" phase at temperature c
K_1	=	"bare" filter resistance to flow
K_2	=	particle layer resistance to flow
M_c	=	mass concentration of Ti vapor in free stream - away from particle
M_x	=	mass concentration of Ti vapor at particle surface
MW	=	molecular weight
Nu	=	Nusselt number
P_{exp}	=	separator chamber pressure
Pr	=	Prandtl number

P_r = reactor pressure

Q = gas volume flow rate at the filter temperature and pressure

Q_c = heat transferred by buffer gas (NaCl) to particle in Δt time

Q_d = heat change for $\Delta m'$ moles of Ti vapor deposited in Δt time step = $(H(Ti, gas, T_g) - H(Ti, refn, T_n)) \times \Delta m'$

Q_p = heat change of particle and coating already on particle (i.e., previous to the time increment) = $(H(B, refn, T_n) - H(B, refn, T_o)) \times$ moles of boron in core of particle + $[H(Ti, refn, T_n) - H(Ti, refn, T_o)] \times$ moles of Ti coating already on particle

Q_r = radiative heat lost by particle to surrounding vessel walls in Δt time = $\sigma' \times A \times \epsilon \times (T_n^4 - T_w^4) \times \Delta t$

Re = Reynolds number

T_a = adiabatic flame temperature

T_g = gas temperature

T_n = particle temperature after a coating time iteration step of Δt seconds

T_o = particle temperature before a coating time iteration step of Δt seconds

T_p = particle surface temperature

T_r = recovery temperature

T_w = coating vessel wall temperature (assumed T_w = 700 K)

U = velocity

a = $D_p/2$

c_g = speed of sound in gas

d_j = jet diameter, 23.5 mm, taken from the thermodynamic equilibrium calculations for an expansion ratio of 15 in this illustration

g = gas phase

h = heat transfer coefficient, = Nu" × k / (2 × a)

h = shock standoff distance = 0.25 × jet diameter, d_j

h_p = specific enthalpy of particle

k = thermal conductivity of buffer gas (NaCl) at gas temperature of T_g

k = rate coefficient of mass deposition per boron particle

k_r = gas thermal conductivity at T_r

l = liquid phase

m = mass of Ti acquired by particle

m′ = moles of Ti acquired by particle

m_p = particle mass

n = natural physical state for substance at pressure and temperature of coating process

r = recovery factor

refn = natural physical state of substance at 101 kPa and specified temperature

s = solid phase

t = time

u_j = jet speed immediately downstream of the shock

v = gas flow velocity at filter face

w = filter mass loading

x = distance along nozzle centerline

$\Delta m'$ = moles of Ti acquired by particle in Δt time step

ΔP = maximum allowable pressure drop across filter

Δt = time step for iterations

γ = ratio of specific heats

γ = average molecular weight

δ = diffusion length taken as the thickness of the velocity boundary layer

ϵ = emissivity of titanium at particle temperature

ϵ = ratio of throat to nozzle area

λ = mean free path, based on viscosity

μ = viscosity

ρ = density

σ' = Stefan-Boltzmann constant

ν_j = kinematic viscosity immediately downstream of the shock

ϕ = equivalence ratio

subscripts:

g = gas
p = particle

SUMMARY

Because of its low mass and high heat of combustion, boron is a very attractive fuel in volume limited, air-breathing engines. Boron has failed to deliver its promised performance because an oxide film on the boron particle surface hinders combustion. It has been proposed that a thin coating of titanium or zirconium would alleviate the problem. In this program, a new process to prepare titanium coated boron particles was evaluated by computer modeling, and an apparatus was designed to prepare titanium coated boron particles.

The new process is based on a process previously demonstrated by AeroChem to prepare pure silicon by reacting sodium with silicon tetrachloride in a rocket motor type system. In that work a photovoltaic grade silicon was prepared at the rate of 1.5 kg/h.

In the new process, sodium is reacted with boron trichloride to produce boron particles and sodium chloride gas. This reaction is exothermic, and in analogy with the silicon process, is assumed to be hypergolic. The reactor resembles a rocket motor and the products are expanded through a nozzle to produce a supersonic stream of boron particles in gaseous sodium chloride and an excess of sodium vapor. The excess sodium reacts with titanium tetrachloride, which is added in the throat of the nozzle or downstream in the expanding section of the nozzle, producing titanium gas which immediately coats the boron particle. The titanium tetrachloride cannot be mixed in the reactor before boron particles are formed because titanium diboride would be formed. The assumption that the titanium coats the boron particle rather than nucleating to form a titanium particle is based on the well known fact that heterogenous nucleation is faster than homogeneous nucleation.

One of the major issues is the collection of very fine particles, 0.5 to 5 μm in diameter. In the silicon process the product is collected as a solid boule. The original concept was to collect the particles on a hot filter, but this seemed cumbersome because of the large quantity of NaCl vapor present. A new method, a supersonic virtual impact collector, was thus conceived. It is the combination of several phenomena. These include the supersonic impact collector used for separating silicon from gaseous sodium chloride, the observation that heavy species are concentrated in the center of a supersonic jet, and the virtual impactor used to classify aerosol particles. Estimates

of the efficiency of this device for separating titanium coated boron particles from gaseous sodium chloride are greater than 95%. The remaining separation would be achieved with a high temperature filter. The gaseous sodium chloride is condensed out as a liquid and removed from the system in the same manner as in the silicon process.

The new process has been analyzed extensively by computer models involving equilibrium thermodynamics; temperature, velocity lag of particles expanded through a supersonic nozzle; and the rate at which titanium coats the boron particles and the increase in particle temperature due to the heat released in coating. The main technical issues are identified as controlling the gas/particle temperatures in the coating operation so that particle temperatures are low enough that the Ti coating remains solid while the gas temperatures are high enough to prevent premature NaCl condensation This analysis required the development of a computer program to calculate the change in particle and gas temperatures during expansion, and the rate of titanium deposition on a boron particle. The information obtained in the modeling work was combined with the design of the silicon apparatus to design an apparatus for demonstrating the process experimentally and producing samples of titanium coated boron particles for evaluation.

1. INTRODUCTION

This is the final report on Phase I of an SBIR the ultimate objective of which is to provide a means of producing Ti or Zr coated boron particles. The coatings will be applied simultaneously with the production of the boron particles to avoid oxidation in handling.

This Phase I program had four tasks:

1. Determine optimum operating conditions for producing Ti or Zr coated boron particles.

2. Determine the range of concentrations required of Ti or Zr chlorides.

3. Evaluate various high temperature filters to be used in separating the product powder from NaCl.

4. Design an apparatus to be built and operated in Phase II.

These tasks have all been completed. In addition, a new means of separating the product powder from the NaCl has been identified and evaluated. We call it a "supersonic virtual impact collector". It will greatly alleviate the problems associated with the envisaged use of high temperature filters. In addition, to make the required optimization calculations, two computer programs were designed and utilized.

The work draws upon the authors' experience in combustion, and specifically in rocket and ramjet technology. It demonstrates the use of combustion technology to produce a valuable product.

Thermodynamic, kinetic, and fluid dynamic calculations were incorporated into computer programs to evaluate the process requirements for producing titanium coated boron powders to meet the specifications identified by King[1] as important for the use of boron for propulsion purposes. An apparatus for the production of the unique coated boron fuel particles was designed based upon the above analysis. In Phase II, the apparatus will be constructed, and coated boron particles prepared for evaluation.

The value of this program is not restricted to the limited application which motivated the work, but has significant implications for other applications

where pure coated metal or composite powders would be useful. One such application would be the relatively (at least in this country) new technique of materials preparation known as SHS (solid high temperature synthesis). In this process, two or more solid particles are mixed together and ignited. A superior product should be produced if the reactants are intimately mixed, e.g., coating one of the reactants with the other.[2]

In this report, we present the background motivating this endeavor, discuss the three computer models which were employed in evaluating the process, present some of the results, describe the new supersonic virtual impact collector, and finally describe the design of the apparatus which will be constructed in Phase II.

2. BACKGROUND ON REQUIREMENTS FOR PROCESS

2.1 BORON PROPELLANTS

Because of its low mass and high heat of combustion, boron has long been considered to be a fuel of choice for both solid and slurry combustors in ramjets or other volume limited, air-breathing systems. However, incomplete and inefficient boron combustion degrades performance in such applications and boron has failed to deliver its promised performance.[3] To overcome this and other difficulties, there is a need to develop improved pure boron fuels containing spherical particles with diameters in the 0.5 to 5 μm range. Calculations indicate that this small particle size is required for complete combustion in the short, about 10 ms, residence time in a combustor.

Such boron fuels are not currently available. Most high purity boron powders in use are supplied by overseas sources,[4,5] e.g., the European firm, Starck Chemical. The disadvantages of such non-domestic sources in times of conflict are obvious. Present fuel boron generally contains 4-6% (weight) impurities, mainly as boron oxide and magnesium, resulting from incomplete cleanup of the boron which is produced by reduction of boron oxide with magnesium. Such impurities not only reduce the volumetric heat release of the boron fuel, but also impede the ignition of boron particles in practical combustors. Furthermore, the powders are reduced to the desired size range by grinding, which results in irregular particles, with sharp edges; grinding can also add

impurities to the product. Such irregular particles present processing and handling difficulties.[4] It is not known how impurities in the boron affect factors such as combustion efficiency, fuel processing, or compatibility with binders in solid fuels. It is nearly impossible to determine these effects experimentally without high purity boron powders to establish a baseline.

The presence of an oxide coating, B_2O_3, on the boron particles lengthens ignition and combustion times. The difficulty arises because the oxide has a low melting point (about 730 K) but a high boiling temperature (about 2070 K for 101 kPa vapor pressure). The liquid oxide layer prevents oxygen from reaching the boron except by slow diffusion processes. The boron may diffuse out or the oxygen may diffuse in. For our purposes the difference is unimportant. Thus the oxide coated boron particle takes a long time, on the scale of the available residence time in the combustor, to get sufficiently hot to evaporate off the oxide and reach the ignition temperature of boron. Once the hot particle begins to burn, this difficulty no longer exists since the particle temperature then exceeds the oxide boiling point.

The boron particle must not only be initially oxide free, but must also be protected from oxide buildup during the particle heatup time prior to ignition. Thus, starting with oxide free boron particles is not sufficient. Various protective coatings of boron particles have been considered to overcome the problems created by the oxide. It would be a relatively simple matter to coat the boron with a material that would protect it from oxidation during storage at ambient temperature. However, many materials that would protect the boron at low temperatures would be either quickly evaporated or burned off the particle surface at temperatures much lower than the evaporation temperature of B_2O_3. These materials also lower the volumetric heat release of t .e boron fuel. Thus, although initially oxide free, these particles would build up an oxide coating long before reaching the boron ignition temperature. Their overall ignition time would therefore be excessive.

King[1] has considered coating boron with high boiling temperature materials. He suggests using a combustible metal with a very high boiling but relatively low ignition temperature. The coating would protect the boron from low temperature oxide buildup and, additionally, the heat release from the combustion of the coating metal would heat the particle faster than for an uncoated particle, thus shortening the boron particle ignition time. Two metals suggested by King are titanium, Ti, and zirconium, Zr, with melting

points of about 1950 and 2125 K and boiling points of 3535 and 3850 K, respectively. The melting points of Ti and Zr oxides are high, about 2100 and 2975 K, respectively.

King[1] modeled the ignition of boron particles coated with various thicknesses of Ti and Zr and assumed that the heat released from the coating combustion was used to heat the boron particle. If the boiling point of B_2O_3 was reached before complete burnup of the coating, the boron particle was assumed to have ignited. If the coating was completely consumed before reaching the boiling point of B_2O_3, a model for pure boron particle ignition was then used, starting at the temperature attained in burnup of the coating, to compute the additional time until boron particle ignition. This study showed that the ignition times could be significantly reduced by Ti coatings representing 9 to 17% of the total particle weight. For example, 2 μm diameter particles in a 2200 K environment at 400 kPa pressure would ignite in 0.09 ms compared to 0.90 ms for pure boron, a factor of ten improvement. Such particles would exhibit about 90 to 94% of the heat of combustion of pure boron particles of the same total weight. Similarly, Zr coatings decreased the ignition times compared to uncoated particles but required slightly larger amounts of Zr (20 to 30% weight) with correspondingly lower heats of combustion (81 to 87% of pure boron).

2.2 AEROCHEM SODIUM FLAME SYNTHESIS PROCESS

A process developed at AeroChem[6] for synthesizing pure metals should be applicable to the preparation of boron powders of the required size, spherical shape, density, and purity. This process has been shown to produce high purity silicon in aerosol form with an estimated average particle diameter greater than 3 μm. If boron powders of similar purity and size could be produced using this technology, a significant step toward overcoming the deficiencies in presently available boron fuel powders would be made.

The AeroChem sodium flame synthesis process consists of: reducing a metal halide (e.g., $SiCl_4$) with a reactive metal (e.g., Na) to produce the pure metal (e.g., Si) as an aerosol in a vapor of the halide salt (e.g., NaCl) of the reductant; expanding these through a nozzle to produce a high velocity stream, usually supersonic; and causing that stream to impinge upon a surface, producing a shock wave, such that the aerosol particles strike the surface and are collected and the NaCl gas is diverted and collected on a condenser as a

liquid. This process has been operated in the laboratory at the scale of 1.5 kg/h to produce a very high quality silicon.

In the specific application previously investigated, the silicon aerosol was produced as a liquid and collected in a novel fashion as a consolidated product. This collection method is not applicable to this program because boron is required as a powder. However, based on the results of this Phase I program, it appears that the AeroChem process will effectively produce high quality boron powders; that it can be modified to allow for the in situ coating of fresh boron powders with Ti or Zr; and that the powders can be efficiently collected. If this can be done, the AeroChem process will provide a material which offers the possibility for realizing almost the full performance potential of boron fuel.

3. DESCRIPTION OF PROCESS

The process to be used for producing coated boron powders is based on the highly exothermic reactions of sodium with boron trichloride and titanium (or zirconium) tetrachloride:

(1) $3Na(l \text{ or } g) + BCl_3(g) \rightarrow B(s) + 3NaCl(g)$

(2) $Na(g) + TiCl_4(g) \rightarrow Ti(s) + 4NaCl(g)$

The AeroChem process[6] will be utilized to produce boron powders by the spontaneous reaction of excess sodium with boron trichloride, Reaction (1), in a high temperature, well-stirred reactor, resembling a rocket motor, Fig. 1. Boron will be produced in the reactor as a solid aerosol with the sodium chloride as a vapor. These will be expanded through a supersonic nozzle, and $TiCl_4$ vapor will be injected in the nozzle to react with excess sodium to produce Ti(g). This gas will condense on the boron particle producing a titanium coated boron particle. The coating process is dependent upon the well-known fact that heterogeneous nucleation is very much faster than homogeneous nucleation. Thus we are not concerned with titanium particles forming separately from the boron particles. The titanium tetrachloride cannot be introduced in the reactor where boron particles are being produced

because titanium boride is a very stable compound thermodynamically and would most likely be formed if the two reactions were carried on simultaneously. The solid boron particle is thus formed first and the titanium coats out on the boron in a separate part of the apparatus.

We assume that, in the times involved, the titanium will condense on the particle and not react to produce titanium boride. A thin coating of titanium boride may not be objectionable (it would still form a protective coating but if the titanium were to penetrate the particle, the coating would no longer be effective) yet an energy penalty would have to be accepted. The objectives are pure boron powder ($\geq$ 99.9%), free of surface oxides, with diameters in the 0.5-6.0 μm range. Also, the particles should be spherical, to enhance their flow properties, and fully dense to maximize their volumetric heating value.

The solid particle product will be separated at high temperature from the gaseous sodium chloride by-product which will be condensed and removed as a liquid. The original plan was to separate the particles from sodium chloride vapor on a high temperature filter, but the size of the filter required, which must be maintained at a high temperature, would be cumbersome. A new means of commercial separation of particles from gas was thus conceived.

In keeping with our analogy of a rocket motor as reactor, we use the entrance to a ramjet diffuser to separate and collect the particles, Fig. 1. A shock wave is formed in front of an aperture in a chamber forming a virtual impactor and a pressure is maintained in the collector chamber equal to the pressure behind the shock (close to the reactor pressure) so that particles can penetrate into the collector chamber, but the NaCl(g) will be turned away to be collected on the NaCl condenser as a liquid. The particles will then be collected on a small filter where any NaCl(g) which gets through the virtual impactor will be passed through and subsequently collected as a liquid on a cold surface.

The apparatus, Fig. 1, resembles a rocket motor and a ramjet diffuser, and its performance was modeled using this analogy.

4. DETERMINATION OF OPERATING CONDITIONS

4.1 CONSTRAINTS

Some of the constraints on the process, which led to a large number of computer runs to satisfy all of them, are:

1. Yields of boron and titanium must be high. Thermodynamics indicates that relatively low temperatures favor high yields.

2. Reaction temperatures must be sufficiently high to support combustion.

3. Temperatures must be sufficiently high to maintain sodium chloride in the gas phase, except at the NaCl collector.

4. Temperatures in the system must never exceed the melting point of boron, or the melting point of titanium or zirconium --after they are introduced.

5. Reactions must be carried out under conditions such that titanium boride, (a stable compound) does not form.

6. The particles exiting the nozzle must form a defined supersonic beam so that they can be separated from the sodium chloride gas by the supersonic virtual impact collector

7. The temperature of the sodium chloride collector (condenser) must be controlled to allow liquid salt to be collected and to prevent formation of NaCl aerosol.

8. Materials of construction; determined by safe operating pressures for high temperature operation.

4.2 THERMODYNAMICS

Numerous experimental studies have demonstrated that metal halides react spontaneously with gaseous alkali metals. The reactions are rapid and highly exothermic. The mechanism appears to involve successive halogen abstraction

reactions to produce the alkali halide and the parent metal atom. Since the reactions are extremely rapid, thermodynamics serves as an important consideration in determining the course of the reaction under various sets of conditions.

The adiabatic flame temperatures, T_a, and product compositions were calculated on a desk top computer using the ISP Thermodynamic Equilibrium Program developed by Curt Selph and Robert Hall at the Air Force Astronautics Laboratory, Edwards Air Force Base, California. A computer program was developed under this program to produce graphs automatically from the ISP program output.

The ISP program is ideal for our application because it was designed for rocket performance calculations and includes the capability to handle solid products. The AeroChem process for preparing boron particles coated by titanium or zirconium involves expansion through a supersonic nozzle exactly as in a rocket. The following properties, in addition to T_a and composition, of the expansion process are calculated by the ISP program and are used as input to the two programs discussed below: ϵ, the ratio of throat to nozzle area; ISP, specific impulse, from which the gas velocity is obtained; average molecular weight; γ $(=C_p/C_v)$, and the gas density.

4.3 PARTICLE VELOCITIES AND TEMPERATURES

A computer program was developed for calculating a single particle velocity and temperature during gas expansion through a nozzle. When a single particle moves at the same velocity as a uniform temperature gas flow surrounding it, the heat transfer rate from the particle is proportional to: (1) the difference between the particle's surface temperature, T_p, and the gas temperature, T_g, and (2) the appropriate Nusselt number Nu, a nondimensional heat transfer parameter dependent on the gas properties and particle size (especially the ratio of the mean free path to the particle diameter), and the particle shape. Under some of the conditions of interest in this program, the mean free path for gas collisions becomes comparable to the particle diameter and the particle velocity is less than the gas velocity. In this region, the Nusselt number is a complex expression and simple continuum results are no longer valid. Expressions for Nu appropriate for this nearly free molecular flow regime were used.[7] In this regime Nu becomes inversely proportional to the mean free path.

The relevant temperature difference is also more complicated than just (T_p - T_g), and is expressed as (T_p - T_r) where the recovery temperature, T_r, is always greater than T_g. T_r differs from T_g when the gas and particle velocities are unequal. T_r includes effects due to viscous and thermal boundary layer transport and adiabatic compression as the slip velocity stagnates on the particle.

The mathematical model used in design of the computer program is summarized here. The particle velocity was calculated based upon the following basic equations:

$$m_p \frac{d\vec{U}_p}{dt} = -\frac{1}{2} \rho_g |\vec{U}_p - \vec{U}_g| (\vec{U}_p - \vec{U}_g) \pi \frac{D_p^2}{4} C_D \quad (1)$$

$$m_p = \frac{4}{3} \pi \left(\frac{D_p}{2}\right)^3 \rho_p \quad (2)$$

$$\frac{dU_p}{dt} = U_p \frac{dU_p}{dx} \quad (3)$$

For subsonic values of $|U_p - U_g|$ the following expressions and experimentally obtained constants were taken from Millikan.[8]

$$C_D = \frac{24}{R_e \alpha} \quad (4)$$

$$\alpha = 1 + \frac{\lambda}{a} (A + B e^{-Ca/\lambda}) \quad . \quad (5)$$

A = 0.874
B = 0.35
C = 1.7

$$R_e = \frac{\rho_g |\vec{U}_p - \vec{U}_g|}{\mu_g} D_p \tag{6}$$

For heat transfer the following equations were used:

$$\frac{\lambda}{a} = 2.52\sqrt{\gamma}\,\frac{|U_p - U_g|}{c_g R_e} = \textit{Knudsen number} \tag{7}$$

$$\frac{d}{dx}U_p^2 = \frac{-36\,\mu_g\,(U_p - U_g)}{\alpha\,\rho_p\,D_p^2} \tag{8}$$

$$m_p \frac{dh_p}{dt} = Q = \pi\, D_p k_r (T_p - T_r)\, N_u \tag{9}$$

$$\frac{dh_p}{dt} = U_p \frac{dh_p}{dx} = \frac{6\, k_r\,(T_p - T_r)\, N_u}{\rho_p\, D_p^2} \tag{10}$$

$$T_r = (1 - r)\, T_g + r T_g^{\circ} \tag{11}$$

$$T_g^{\circ} = T_g\left[1 + \frac{\gamma - 1}{2} M_{rel}^2\right] \tag{12}$$

$$M_{rel} = |U_p - U_g| / c_g \tag{13}$$

$$r = \sqrt{P_r} \tag{14}$$

$$N_u = \frac{\bar{N}_u}{1 + 3.42\,(M_{rel}/R_e\, P_r)\,\bar{N}_u}; \quad \textit{valid for } M_{rel} \leq 1 \tag{15}$$

$$\bar{N}_u = 2 + (0.4\, R_e^{1/2} + 0.06\, R_e^{2/3})\, P_r^{0.4} \left(\frac{\mu_r}{\mu_p}\right)^{1/4} \tag{16}$$

Curve fits were used to obtain:

$$h_p = h_p\,(T_p)$$
$$\mu_g = \mu_g\,(T_g)$$
$$k_r = k_r\,(T_r)$$

A computer program was developed to calculate particle temperature and velocity based on the above mathematical model. In this analysis we treat the effects of velocity slip between the particle and the gas and a finite gas mean free path. The computer program solved (numerically) the two first-order differential equations (Eqs. 1 and 9) for particle enthalpy (temperature) and particle velocity. Input nozzle flow properties, e.g., gas velocity and temperature, and the chemical composition as a function of distance along the nozzle centerline were obtained from the ISP program. The particle velocity and temperature computations are based on the approximation that all condensed phase material is sufficiently finely divided that its temperature and velocity are the same as that of the gas, except for a single test particle of fixed size, whose temperature and velocity are calculated. There is thus some ambiguity in applying this program to an ensemble of particles; the total enthalpy computed in the ISP program is that of particles and gas in thermal equilibrium, while in practice, the distribution of enthalpy between particles and gas is determined by the heat transfer mechanism used in this calculation. Thus the gas temperatures taken from the ISP program and used in the calculation will be greater than in practice. The calculated rates of particle cooling on expansion will thus be slower than in reality because $T_p - T_g$ in the model calculation will be less than reality. This is a conservative calculation. Increased cooling of the particle, as will be seen below, is important.

4.4 RATE OF GROWTH OF PARTICLE SURFACE COATING

The basic equation for calculating the rate at which Ti vapor molecules deposit onto a growing boron particle surface is:

$$\frac{dm}{dt} = A \times k \qquad (17)$$

where k is the rate coefficient of mass deposition per boron particle.

When the coating process is described by continuum fluid mechanics, a simple relationship can be derived for the rate coefficient[9] .

$$k = D \times \frac{(M_c - M_x)}{a} \tag{18}$$

The value of M_c is obtained from the ISP calculation constrained to produce only gas phase titanium. This is an artificial device for imposing a kinetic restriction on an equilibrium calculation. The assumption is that titanium vapor is first formed, and because heterogeneous nucleation on the boron particle is infinitely rapid compared to homogeneous nucleation, the titanium or zirconium will solidify only on the boron particle. The value of M_x is taken to be that established at the equilibrium vapor pressure of Ti or Zr at the current temperature of the particle. The relationship between Ti vapor pressure and temperature was found by fitting data reported in Refs. 10 and 11.

The coating simulation calculation is performed by a finite difference method, that is, we calculate the moles (m′) of Ti deposited in a small time increment:

$$\Delta m' = \frac{A \times k \times \Delta t}{MW} \tag{19}$$

From the moles deposited on the particle in this time increment, the heat gains/losses for the coating system are balanced by iteration on T_n. The heat balance equation is:

$$Q_p = Q_d + Q_c + Q_r \tag{20}$$

The heat gained by the particle is equal to the heat transferred to the particle by the condensation of Ti vapor, heat transferred to/from the buffer gas, and the loss of heat from the particle through radiation. Note that Eq. (20) assumes that the particle has infinite thermal conductivity, i.e., that it instantly distributes incoming heat throughout its entire mass. There is some theoretical evidence in our calculations that this does not occur; boron is a poor thermal conductor.

In the next, and subsequent, time steps, T_n is used as the starting particle temperature. The gas temperature, particle radius (for the amount of Ti coated) and drop in Ti vapor concentration are all updated before each time step in this calculation.

In the finite difference approach, if the time increment, Δt, is made too large the calculations will yield very crude approximations to the actual coating process. However, by simply making Δt smaller, and observing the results, it can be verified that the Δt value chosen is sufficiently small. In this case, the step size was judged to be sufficiently small when the results did not change by more than about 1% when the Δt step size was decreased by a factor of two.

The thermodynamic data were taken from the JANAF tables. Self diffusion coefficients; coefficients of diffusion of Ti(g) in NaCl(g); viscosity; and thermal conductivity were calculated over the required temperature range following procedures employed in Ref. 12.

4.5 RESULTS

A large number of computer runs was made to arrive at a set of operating conditions which meet all of the constraints (Section 4.1) on the process. This research program could not have been performed without the availability of inexpensive computer time such as a desk top computer offers; laboratory experiments could never be justified without first examining the possibilities by computation. We report only on some of the results, notably those which are most definitive in determining the experiments to be performed in Phase II.

Calculations have been made based upon the sodium feed in the vapor phase, in the liquid phase, and mixtures of the two phases. The possibility of using magnesium instead of sodium has also been considered. The most significant challenge has been to define a set of conditions under which the particle temperature does not attain the melting point of the coating metal, Ti, and yet the gas temperature is sufficient to maintain the sodium chloride in the vapor phase. Prior to initiating experiments, additional computer runs should be made in which the two programs for calculating the particle temperature and velocity and the rate of deposition of titanium on the boron surface are coupled. In our initial thinking about this process, we underestimated both

the importance of particle heating due to deposition of a coating and the sensitivity of the particle temperature to gas-particle fluid mechanical coupling. A large quantity of energy, the heat of fusion, is transferred to the particle when it is coated and the rate of heat transfer from the particle to the gas is very slow. The rate of equalization of temperature throughout the particle should also be incorporated into the calculation; it may, in fact, enhance the rate of heat loss from the particle to the gas.

4.5.1 General Considerations

Thermodynamic calculations for Reaction (1) are presented in Figs. 2 to 7. Except where specified, the reagent ratio is stoichiometric (the equivalence ratio, ϕ, = 1.0 or Cl/Na = 1), the reactor pressure, P_r, = 25 kPa and the separator chamber pressure, P_{exp}, = 2 kPa. The data reported in Figs. 2 to 7 are based on adiabatic thermodynamic equilibrium calculations, i.e., ISP calculations, in which various parameters such as Cl/Na ratio, initial pressure, pressure ratio between the reactor and separator chamber, frozen or shifting equilibrium nozzle expansion, and reactor temperature (controlled by heat loss or diluents), have been varied to ascertain their influence upon adiabatic flame temperature and boron yield.

Shifting and frozen flow represent the two extremes for the reaction rates during expansion. In the shifting equilibrium case, the chemical reaction rates are infinitely fast compared to the flow time in the nozzle; frozen flow is the other extreme, the reactions are infinitely slow compared to the flow time. The kinetics of the process determines the condition between these extremes. In our work with silicon, the experimental results were close to the shifting equilibrium case.

These figures indicate those conditions for which high yields of boron are expected. Figure 2 shows the reaction temperature is not sensitive to the Cl/Na reagent ratio. Figures 3 and 4 show the stability of the BCl; other products were less than 0.01 mole fraction. When the phase of a chemical species is not indicated, it is in the gas phase. In Fig. 3, boron is indicated as liquid or solid. In the reactor it is liquid; it may or may not solidify in the nozzle when the gas temperature falls below the melting point, depending upon the rate of heat transfer from the boron droplet to the gas phase. In subsequent calculations, it was determined that heat transfer from the boron aerosol to the gas was very slow, so that reactor conditions had to

be chosen in which the aerosol was a solid and not a liquid. The boron yield increases, Fig. 5, with excess of sodium (no heat losses) but is still lower than desired. The temperature in the reactor is artificially controlled in Fig. 6 for a stoichiometric mixture. This can be done, e.g., by dilution, controlling the heat loss, or heating reactants. The yield of solid boron is about 60% of the input BCl_3 at the adiabatic flame temperature, 2510 K, and this yield increases rapidly to $\geq$ 95% as the temperature is reduced to 2100 K. In the exhaust of the reactor, the exit nozzle in our rocket motor analogy, the boron yield is increased as the temperature decreases and the equilibrium composition changes, as shown in Fig. 6 by the line labeled "SHIFTING". Figure 6 thus indicates that for a stoichiometric mixture, 100% yield can be obtained by reducing the flame temperature. It is recognized, of course, that if solid particles are formed from cooling in the expansion, nearly the reactor temperature will be recovered when they strike a surface, e.g., the particle filter, so that energy will have to be extracted from the exhaust stream before it strikes a surface. Previous experience indicates that with a poorly designed nozzle this readily occurs through mixing with exhaust gases when shock waves (Mach diamonds) are formed.

Figure 7 demonstrates the effects on boron yield of changing the reactor pressure and the expansion pressure. The yield increases with reactor pressure and with increasing pressure ratio. This may be more of a temperature than a pressure dependence.

When either $TiCl_4$ or $ZrCl_4$ were added to the reactor in realistic quantities to coat the boron particles, $TiB_2(s)$ or $ZrB_2(s)$ was produced. This is clearly undesirable so that later computer experiments were done by adding the titanium tetrachloride in the nozzle throat or in the nozzle downstream of the throat, see Fig. 1. The results of one of these sets of calculations are shown in Figs. 8 and 9. In this example, the reactor was operated at 101 kPa and the titanium tetrachloride was injected into the nozzle after the products from the reactor had been expanded to 50 kPa. By using liquid sodium feed instead of gaseous sodium, the temperature was maintained sufficiently low that solid boron was formed immediately in the reactor. In this run we also operated at 10% excess sodium which suppressed the $TiCl_2$ concentration below 0.0005 mol fraction. The Ti(s) produced would be expected to coat out on the boron particles.

4.5.2 Design Conditions

In this section we report on the results which indicate the feasibility of the process and at this stage represent the best set of conditions at which to initiate laboratory experiments. Some fine tuning will be required prior to initiating experiments.

The results of the ISP program thermodynamic calculations are reported in Figs. 10 to 14 with $TiCl_4$ injected in the throat of the nozzle. We chose to inject the coating reactant in the throat because mixing should be better there with minimal disturbance to the integrity of the jet, and because it is the lowest temperature at which the reactant could be injected without B- and Ti-forming reactions occurring in the same reactor space and probably producing TiB_2.

Figure 10 presents the variation of shifting and frozen equilibrium temperatures. Our experience with silicon has indicated that shifting equilibrium dominates in that system. Reaction rates will determine the temperature to be between these two extremes. We have generally chosen to consider the shifting flow case, the worst case for meeting the constraint of maintaining the titanium on the boron particle in the solid phase. The frozen flow case would be the worst case for maintaining the sodium chloride in the gas phase. In Fig. 11 the pressure as a function of distance from the nozzle throat is compared with the vapor pressure of NaCl determined by shifting equilibrium temperature of the gas from Fig. 10. Beyond about 12 cm the NaCl would condense out.

The equilibrium concentrations of products are shown in Figs. 12 and 13. The yield of boron is 100% throughout the whole system, Fig. 14. Titanium concentration increases rapidly with expansion ratio--remember this is equilibrium--reaching greater than 70% yield and then rising rapidly to about 98% yield. It of course levels off because it is depleted. We will see below that a slower rate of titanium production may be desirable to minimize the rate of temperature rise of the particle.

The results of the particle temperature, velocity calculations for the above equilibrium calculations are presented in Figs. 15 to 18 for 1 μm and 6 μm diameter initial boron particles. The temperature of the 1 μm particle, Fig. 15, lags several hundred degrees behind the gas temperature. The nozzle entrance and expansion angles have already been decreased to increase the time

scale so that both half angles are 2°. It would be desirable for these two temperatures to be close together, that is a lower particle temperature to prevent Ti from liquefying on the boron particle and a greater gas temperature, to prevent NaCl from condensing. Figure 16 shows, as expected, that the temperature of a 6 μm particle lags the gas temperature even more.

The velocity lag for the 1 μm particle is very small, Fig. 17, so that for all practical purposes the particle may be considered to be at the local gas velocity. However, for the 6 μm particle, Fig. 18, the lag is significant and must be taken into account in the particle growth and heat transfer calculation.

The rates of growth for 1 and 6 μm particles are shown in Figs. 19 and 20. The diameter required for a 10 weight % coating would be 1.017 and 6.10 μm for a 1 and 6 μm initial boron particle, respectively. For the 1 μm particle the limiting diameter is determined by the melting point of titanium, Fig. 21. For the 6 μm particle the limiting diameter is determined by the NaCl gas temperature reaching the condensation temperature of NaCl, Fig. 22. Thus the conditions for the process will be varied depending upon the size of boron particles produced. The reaction rates controlling the production of boron particles and the rates of coagulation are not sufficiently well known to use them in making such calculations. These rates may be deduced from our Phase II experiments. We do know, however, how to alter the experimental conditions to control the particle size. Thus when the particle sizes are determined in a specific experiment and it is desirable to increase or decrease them, we know what experimental parameters to change and in which direction.

The calculated range of limiting conditions, above, should be broadened by combining the two computer programs which now separately calculate particle temperature/velocity and particle growth/temperature increase due to coating metal deposition. The coating process is very exothermic, about 460 kJ/mol at 1500 K. The condition is exacerbated by the low heat transfer coefficient for NaCl gas, 8 mW/M/K at 500 K. This could be increased by adding a high thermal conductivity gas to the system, e.g., He. The heat transfer for He at 500 K is 2,000 mW/M/K, 250 times that of NaCl gas. Thus in the fine tuning of the system prior to initiating Phase II experiments, we will perform some calculations in which helium is either added in the reactor or in the nozzle throat with the $TiCl_4$. The implications of this are, of course, a requirement for minimal pumping capacity with helium addition. Some is already required by the supersonic virtual impact collector. Because all of the products and by-

products are solids the helium could very easily be cycled through the system. It would only have to be pumped from the low pressure chamber to the reactor pressure.

5. APPARATUS DESIGN

This section concerns the apparatus design. The reactor and feed systems are largely based on our previous experience with silicon preparation. The major issue in this program is the collection of small particles rather than a consolidated material. This is an even greater challenge than usual because the particle collection system must be maintained above the boiling point of sodium chloride everywhere except on the NaCl condenser. Since the apparatus design work was pursued simultaneously with the process optimization studies, and some of the basic design parameters differ in the two studies, e.g., in the process optimization studies, a reactor pressure of 50 kPa with a combined Na(g)/Na(l) feed was considered while in the apparatus design work, a reactor pressure of 25 kPa and Na(g) feed was considered, some of the basic design parameters differ in the two studies. This does not represent a problem; prior to initiating construction in Phase II the differences will be reconciled. They do not alter the feasibility of the process.

5.1 REACTOR AND FEED SYSTEMS

The apparatus has been chosen to be as small in scale as possible consistent with a reactor nozzle diameter large enough to avoid clogging and to simplify heat control problems. Based upon our work with silicon we estimate a reasonable minimum nozzle throat diameter to be about 0.5-0.6 cm. The most conservative estimate for the reactor nozzle assumes minimum gas flow, i.e., that we are producing pure, uncoated boron (only the BCl_3 + 3Na reaction takes place) in the reactor. Adding the amount of Na required to react with $TiCl_4$ or $ZrCl_4$ downstream of the nozzle, the product gas from the reactor consists of 3 moles of NaCl for each mole of boron plus [4 × X_c × (number of moles of boron)] moles of Na, where 4 is the stoichiometry required to convert $TiCl_4$ (or $ZrCl_4$) to free coating metal vapor, and X_c is the mole fraction required to give a coating of the "appropriate" thickness. Appropriate thicknesses were chosen based on the work of King[1] who suggests Ti coatings in the 9-17% mass

fraction range and Zr coatings in the 20-30% mass fraction range. For fully dense particles, these ranges correspond to coating thicknesses in the range of 2-3.5% of the particle radius for Ti coatings and 3-5% of the particle radius for Zr coatings. For both coating metals, $0.03 \leq X_c \leq 0.05$. Thus, the flow from the reactor consists of 3.12 to 3.2 moles of gas for each mole of boron produced. We chose a 0.3 kg/h production rate of boron particles at a reactor pressure of 25 kPa with a 0.6 cm diameter nozzle for the design condition.

Higher reactor pressures would require special materials (e.g., zirconium alloy) if sodium vapor were used. The above thermodynamics indication that liquid sodium can be used allows us to work at higher pressures without special materials.

Table 1 lists some design parameters for a 0.3 kg/h laboratory scale coated boron powder production apparatus operating at a reactor pressure of 25 kPa. A process and instrumentation diagram is presented in Fig. 23. Some detailed designs are presented in Figs. 24 to 28. Detailed dimensions are not always provided but the figures are generally to scale, are in a CAD program, and so can be easily modified to exact machining dimensions prior to initiating construction in Phase II.

5.2 PARTICLE SEPARATION

As pointed out above, one of the major issues in this program is the collection of very hot small particles. We have previously considered several techniques of doing this.[13,14] When this program was proposed, we considered using hot ceramic type filters. During the course of this work, the hot filters required to do the job appeared to be excessively large, so we considered other techniques and came upon the idea of a supersonic virtual impact collector described below. This is a combination of three experimentally demonstrated technologies; concentration of the heavy species in the core of a jet, the AeroChem supersonic impact particle separator, and a supersonic virtual impact collector. Should this work as well in practice as it seems to on paper, its demonstration would be a significant contribution to the general subject of particle collection.

5.2.1 Supersonic Virtual Impact Collector

Product coated boron particles will be separated from NaCl vapor using a supersonic virtual impact collector,[15] Figs. 1 and 29. The basic principles governing the separation of product particles from by-product gas are very similar to those for the impactors used previously in our silicon work. The unique new features are: (1) taking advantage of the fact that under appropriate conditions the heavy species remain concentrated in the core of a high velocity jet while the lighter species diffuse out of the jet, and (2) after the jet is caused to produce a shock wave by impacting the virtual impact collector face plate containing an aperture, Fig. 29, letting the particles flow through the aperture into a chamber maintained very close to the pressure downstream of the shock, where they are collected by conventional techniques, e.g., a filter.

Under appropriate conditions in an expanding jet, particles will concentrate on the centerline of the jet. Haegele[16] has shown that de Laval nozzles can form aerosol beams in which particles are focused into a core due to the fact that outward radial acceleration of the particles is smaller than that of the gases.

The ability of the particle trajectories to follow or separate from gas jet streamlines determines the focusing effect, and consequently particle size will be important. In Phase II work, the phenomena will be analyzed and modeled in more detail to optimize nozzle design for particle focusing.

For present design purposes, we assume that we can achieve Haegele's focusing result, i.e., the particles concentrate into a core of approximately half the exit diameter with a small divergence angle.

The concept for the supersonic virtual impact collector is taken from the literature of particle measurements where such devices are used to separate particles according to their sizes. In these devices a subsonic gas stream containing particles is caused to impinge upon a surface containing an aperture. By maintaining a gas pressure behind the aperture equal to the pressure of the impinging stream, the gas in the jet and the small particles which follow the gas flow are inhibited from entering the aperture, but larger particles, with greater momentum, will enter. Very accurate and balanced control of the two pressures on either side of the aperture prevent convective flow, so that the only transport of gas across the aperture will be by diffusion.

For our work, we will combine the virtual impact collector concept with the supersonic jet we have previously used to form a shock wave in front of a particle collecting surface. In this jet, even small particles such as those we wish to collect have sufficient momentum to deviate from the gas flow streamlines behind the shock. The gas behind the shock is at nearly the pressure in the reactor so that if the aperture of the virtual impact collector is placed behind the shock, Fig. 29, and sufficient gas pressure is maintained in the impactor chamber, the particles in the jet will enter the aperture and the gas in the jet will flow to the side.

For design purposes, the aperture in the virtual impact collector was chosen to be the particle beam diameter, assumed to be 0.75 cm, i.e., 0.15 cm larger than the nozzle throat diameter (0.6 cm); this allows for some particle beam divergence. A conical shape was chosen for the virtual impact collector, with an included angle of 120°, so that the shock standoff distance is reduced compared to what it would be with a flat surface. Inert gas, e.g., Ar, is introduced through a porous tube into the impactor chamber, Fig. 29, to maintain the pressure in the impact chamber slightly greater than the pressure behind the shock wave. The Ar flow is divided: a small part moving toward the impactor aperture and the bulk being pumped in the opposite direction toward a filter to collect coated particles. Assuming that the recovery pressure is 25 kPa (reactor pressure) and that the temperature of the Ar in the virtual impact collector is about 1400 K (see below), 3 μm diameter boron particles moving at 100-500 m/s will penetrate[17] about 3.2 to 14 cm behind the shock before slowing to their gravitational settling velocity. To obtain the pressure balance desired without flow disturbances it is necessary to minimize the flow perturbances in the virtual impact collector chamber. This has been achieved in a subsonic virtual impact collector by using a porous wall tube to introduce the inert flow behind the impactor aperture.[15] The porous tube was axially aligned with the particle jet and the inert gas flow through the tube walls was adjusted to obtain proper flow balance.

The amount of inert gas needed to maintain the virtual impact collector is small--the flow velocity toward the particle filter should exceed the settling velocity of the particles to increase the rate of filtration. For the 25 kPa, 1400 K condition, the settling velocity[17] of 3 μm diameter particles is about 0.05 cm/s. To be conservative, we assume a gas flow velocity of about 2 cm/s to transport the particles to the filter. Using a filter area of 0.24 m^2 (about 2 ft in diameter, see below), an Ar flow of 0.2 standard (101 kPa, 273.2 K) L/s is required to achieve this velocity.

An estimate of the degree of separation of NaCl from particles at the virtual impact colector was obtained by computing the flux of NaCl vapor across the plane of the aperture of the virtual impact collector, assuming that diffusion is the only process involved. Thus[18]:

$$F = D\,(C_2 - C_1)/\delta \qquad (21)$$

Equation (21) was evaluated at the recovery conditions behind the shock, assumed to be those of the reactor: T = 1900 K, P = 25 kPa. For these conditions, D = 10.4×10^{-4} m^2/s. The NaCl concentration, $C_2 = 9.7 \times 10^{23}$ molecules/m^3 and $C_1 \equiv 0$ (i.e., the maximum gradient is assumed so that this is a worst case calculation). The diffusion length, δ, was taken to be equal to the thickness of the velocity boundary layer which would exist if the impactor surface were solid:

$$\delta/h = 6.39\sqrt{\nu_j/u_j d_j} \qquad (22)$$

The functional form of Eq. (22) results from a standard analysis of boundary layer growth in stagnation flows,[19] and the constant results from an analysis of data on impinging jets.[20] Equation (22) gives $\delta \approx 0.1$ cm and Eq. (21) gives $F = 1 \times 10^{26}$ molecules/m^2-s. The area of the virtual impact collector aperture, A_i is taken as 4.4×10^{-5} m^2 (diameter = 0.75 cm, see above). Thus, $FA_i \approx 5 \times 10^{10}$ molecules/s (0.08 mmol/s) enter the virtual impact collector. The net flow of NaCl from the reactor and coating process is (Table 1) 31 mmol/s, so that (0.08/31) × 100 ≈ 0.3% of the NaCl produced in the reactions enter the impactor with the coated particles; the calculated separation efficiency is thus > 99%.

5.2.2 Hot Particle Filter

The coated boron particles will be collected downstream of the virtual impact collector separator using a filter. The flow through the filter is comprised of particles suspended in Ar and a residual amount of NaCl vapor (see above). We estimate the size of the filter required and the amount of Ar needed as follows: As a conservative design estimate, we assume that 5% of the NaCl produced in the reactions (0.05 × 31 = 1.55 mmol/s = Q_{NaCl}) gets into the

impactor chamber downstream of the virtual impact collector. This amount of NaCl will be contained in sufficient Ar to maintain the flow velocity through the filter at ≥ 2 cm/s (for particle transport as indicated above), and the total gas flow, Q_{tot}, will be sufficiently hot that NaCl condensation does not occur at a total pressure, P_{tot} = 25 kPa. The condition for no condensation can be written as:

$$(Q_{NaCl}/Q_{tot})\,P_{tot} < P_{sat} \qquad (23)$$

i.e., that the partial pressure of NaCl must be less than its saturation vapor pressure, P_{sat}, in the flow. Equation (23) may be recast

$$Q_{Ar} > Q_{NaCl} \times (P_{tot}/P_{sat} - 1) \qquad (24)$$

from which we can obtain the minimum Ar flows required at various operating temperatures (to maintain P_{sat}). The filter area, A_f, is obtained from the requirement that the flow velocity, $v \geq Q_{tot}/A_f$, where Q_{tot} is now expressed in volume units/s at P_{tot} and the operating temperature using the perfect gas law. Table 2 diplays the values of Q_{tot} and A_f computed using Eq. (24) and the velocity condition with Q_{NaCl} = 1.55 mmol/s and for temperatures up to 1560 K (where P_{sat} = 25 kPa--the collector could be operated above this, but we prefer to operate at as low a temperature as possible).

The values in Table 2 suggest that a reasonable design temperature for the filter collector is about 1400 K with an Ar flow in the range 0.15-0.2 standard L/s and a filter area of 0.18-0.25 m^2. Lower collector temperatures demand excessive Ar flows and filter areas.

The temperature requirements indicate that ceramic or graphite filter materials will be required. Commercial ceramic plate filters are available from Selas, Inc. (Selas Micro-Porous Porcelain, 0.2-0.5 cm thick, continuous use to 1600 K with retention capabilities to submicron particle sizes).[21] In a plate, or surface filter such as this, particles are collected at the surface with little or no penetration. Fabric or fiber filters, e.g., Nextel fabric from 3M (Nextel 312 woven fabric, AF style, continuous use up to 1500 K, 0.036-0.12 cm thick)[22] allow particle penetration and their main filtering action takes place after a layer of particles builds up on them. The layer

buildup and filtering efficiency are favored by low gas flow velocities such as required here.

The power required to heat the Ar flow from room temperature to 1400 K is about 200 W. For the initial experimental apparatus of Phase II, the Ar flow will be separately preheated, but in a commercial device it is likely that preheating will be accomplished in part by tapping off part of the coolant gas from the main salt collector. Radiant graphite rod heaters of the kind we have used previously in our silicon synthesis work will be used in the experimental program.

The basic engineering equation for filter performance is given by Perry:[23]

$$\Delta P = K_1 v + K_2 w v \qquad (25)$$

We use Eq. (25) to determine the time between filter "cleanings" by mechanical agitation. For fabric filters, $K_1 \approx 0$, and $P \approx K_2$ w v. For the ceramic porous plate filters, K_1 is non-negligible. Values of K_1 depend primarily on pore size and filter thickness[10]; K_2 depends primarily on particle size and shape (i.e., on "packing" in the filter cake). Values of K_2 increase with decreasing particle size. Values of $K_{1,2}$ are usually given for air at 273 K and are corrected for other filter gases and temperatures by multiplying by the viscosity ratio of the actual filter gas to that of air (0.018 cps). We used Eq. (25) to compute w for the filters at the 0.3 kg/h coated particle production rate.

We consider first the case of a fabric filter: For 2 μm diameter particles (carbon black), Perry[23] gives K_2 = 466 (K_2(1400 K, Ar/NaCl mixture) = 1540); thus, to obtain the maximum pressure drop (worst case) of 25 kPa, w = $\Delta P/(K_2$ v) = 0.8 kg/m^2. From other work at AeroChem, we have found that 3 μm diameter boron powders exhibit a tap density of ≈ 1000 kg/m^3; the maximum mass loading thus corresponds to a filter cake thickness of ≈0.01 cm. Thus, we predict that a 0.24 m^2 fabric filter will achieve a pressure drop of 25 kPa after collecting 0.192 kg of particles. This corresponds to an operating time of 0.5 h between cleanings.

For the ceramic plate filter from Selas, K_1 = 180 for a 1.5 μm diameter rated filter (K_1 (1400 K, Ar/NaCl mixture) = 650) giving w = 0.4 kg/m^2 for ΔP= 25

kPa and a time between cleanings of 0.3 h. Clearly, both predicted values for times between cleaning are sufficiently small that continuous agitation or vibration of the filter will be desirable. The filter will be mounted in a vertical position to allow the product particles to fall into an accumulator. In terms of standard filter practice, this will allow us to utilize either "bag" filters of fabric or rigid "candle" filters of porous ceramic. Based on the longer times between cleaning, cost, and ease of use, the fabric filter appears more desirable than the ceramic plate filter. The fabric filter will have an initial startup loss until particles build up within the fabric; according to Perry, after the first cleaning, this internal buildup remains partially intact (i.e., $K_1 > 0$, but smaller than for surface filters) and losses between cleanings are reduced from the virgin filter condition.

6. PATENTS

AeroChem plans to file for a patent on the coating process as a generic process for coating particles, and on the supersonic virtual impact separator as a generic process for separating small particles.

7. REFERENCES

1. King, M.K., "Modeling of Effects of Various Aids (Halogens, Metal Coatings, LiF Coatings) on Boron Particle Ignition," 21st JANNAF Combustion Meeting, CPIA 412, Vol. II, 1984, p. 37.

2. Holt, B., Lawrence Livermore Laboratory, personal communication, September 1989.

3. Faeth, G.M., "Status of Boron Combustion Research," 21st JANNAF Combustion Meeting, CPIA 412, Vol. I, 1984, p. 15.

4. Nieder, E.G., Atlantic Research Corp., private communication to W. Felder.

5. Janson, L., Callery Chemical Co., private communication to W. Felder.

6. Felder, W. and Calcote, H.F., "A Sodium Flame Process for Synthesis of Pure Metals and Ceramics," AeroChem TP-483, presented at Western States Section/The Combustion Institute Meeting, Pullman, WA, 20-21 March 1989. Patents have been issued in the following jurisdictions: Canada, Europe, France, Germany, Italy, Spain; patent applied for in the United States.

7. Schaaf, S. A. and Chambré, P.L., Flow of Rarefied Gases (Princeton University Press, Princeton, 1958).

8. Millikan, R.A., Phys. Rev. 22, 1 (1923).

9. Felder, W., Madronich, S., Olson, D.B., "Oxidation Kinetics of Carbon Blacks over 1300-1700 K," Energy & Fuels 2, 743 (1988).

10. American Institute of Physics Handbook, 3rd ed., D. E. Gray, Ed. (McGraw-Hill, New York, 1972) p. 6-203.

11. CRC Handbook of Chemistry and Physics, 65th ed., R. C. Weast, Ed., (CRC Press, Boca Raton, FL, 1984) p. D-218.

12. Svehla, R.A., "Estimated Viscosities and Thermal Conductivities of Gases at High Temperatures," NASA TR-R-132, 1962.

13. Felder, W., "Vapor Coating of Boron Fuel Particles by Magnesium," Final Report, AeroChem TP-479, December 1988.

14. Berman, C.H., in Aerosols: Science, Technology, and Industrial Applications of Airborne Particles, B.Y.H. Liu, D.Y.H. Pui, and H.J. Fissan, Eds. (Elsevier, New York, 1984) p. 683; Gould, R.K. and Srivastava, R., "Development of a Model and Computer Code to Describe Solar Grade Silicon Production Processes," AeroChem TP-392, DOE/JPL 954862-79/8, 1979.

15. For example, see Noone, K.J., Ogren, J.A., Huntzenberg, J., Charlson, R., and Covert, D.S., "Design and Calibration of a Counterflow-Virtual Impactor for Sampling of Atmospheric Fog and Cloud Droplets," Aerosol Sci. Techn. 8, 235 (1988).

16. Haegele, J., "Optical Investigation of High Speed Aerosol-Microjets," J. Aerosol Sci. 13, 471 (1982).

17. Friedlander, S.K., Smoke, Dust and Haze (Wiley, New York, 1977), Ch. 2.

18. Crank, J., The Mathematics of Diffusion (Oxford Univ. Press, London, 1951) Ch. 4.

19. Schlichting, H., Boundary Layer Theory, 4th ed. (McGraw-Hill, New York, 1960).

20. Donaldson, C.D., Snedeker, R.S., and Margolis, D.P., "A Study of Free Jet Impingement. Part 2. Free Jet Turbulent Structure and Impingement Heat Transfer," J. Fluid Mech. 45, 477 (1971).

21. Selas Corp. of America, Minnetonka, MN, "Selas Microporous Porcelain Filter Media and Apparatus," Product Bulletin FMA-1, 1988.

22. Ceramic Fiber Products, St. Paul, MN, "Nextel Ceramic Fiber," Product Bulletin K-MHNFOL-1(241)11.

23. Perry, R.H. and Green, D., Perry's Chemical Engineers' Handbook, 6th ed. (McGraw-Hill, New York, 1984) Ch. 20.

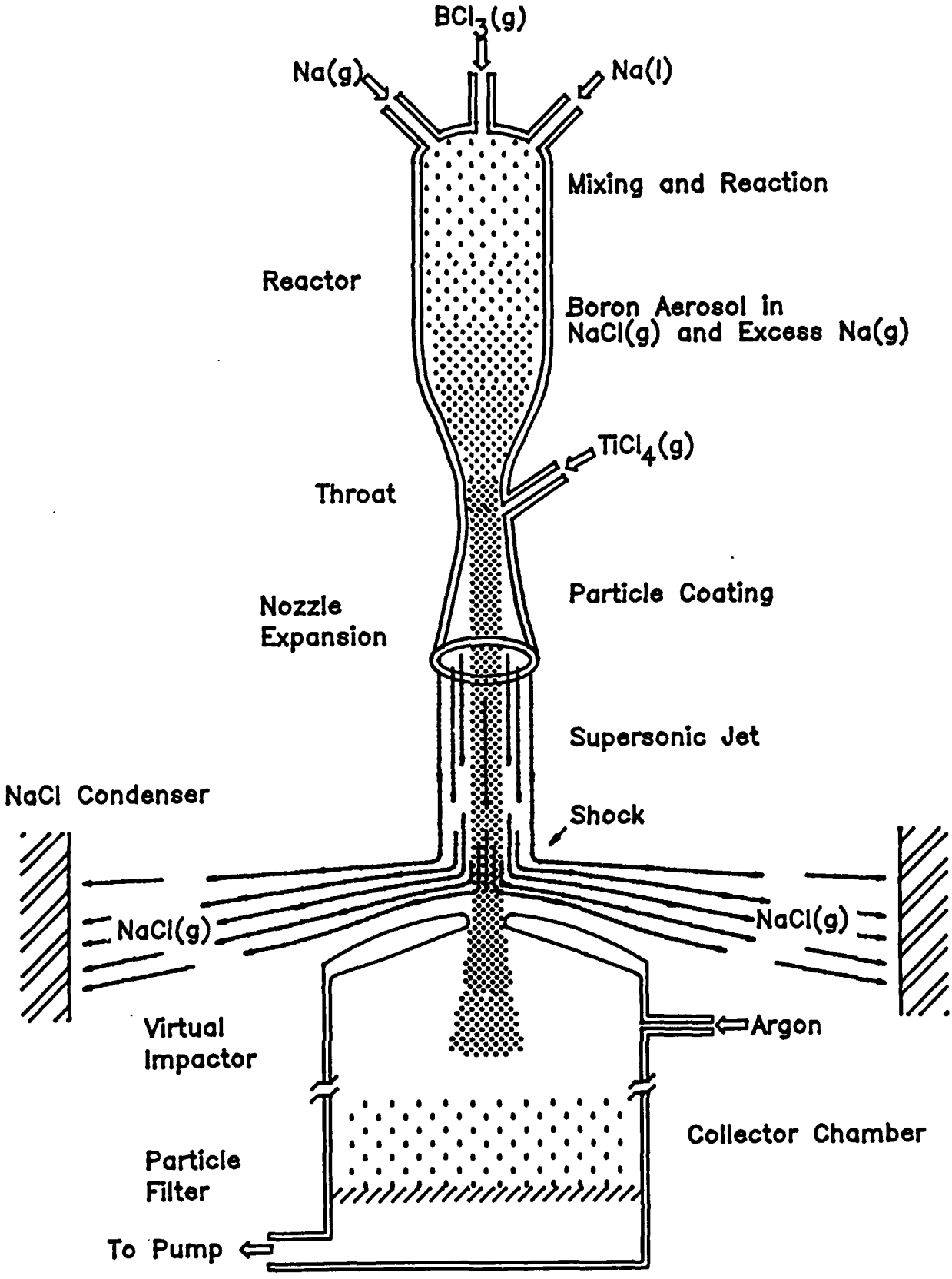

Figure 1. AeroChem process for producing coated boron particles

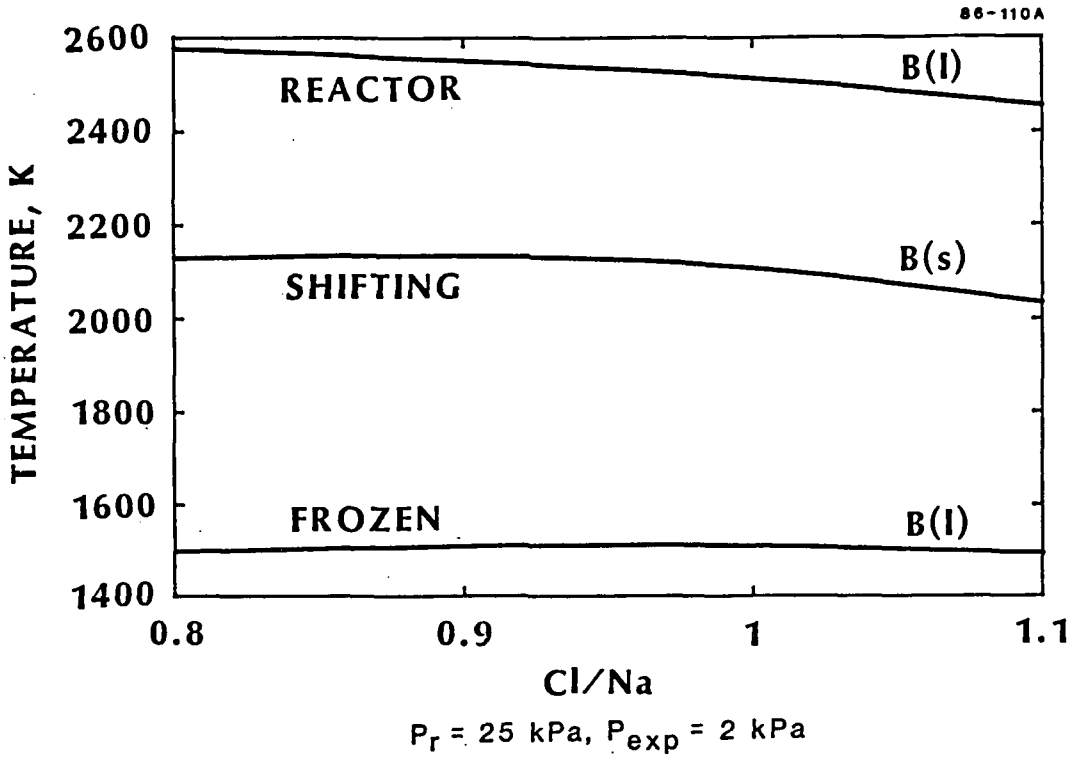

Figure 2. Effect of chlorine sodium ratio on adiabatic reactor, shifting, and frozen flow, temperatures

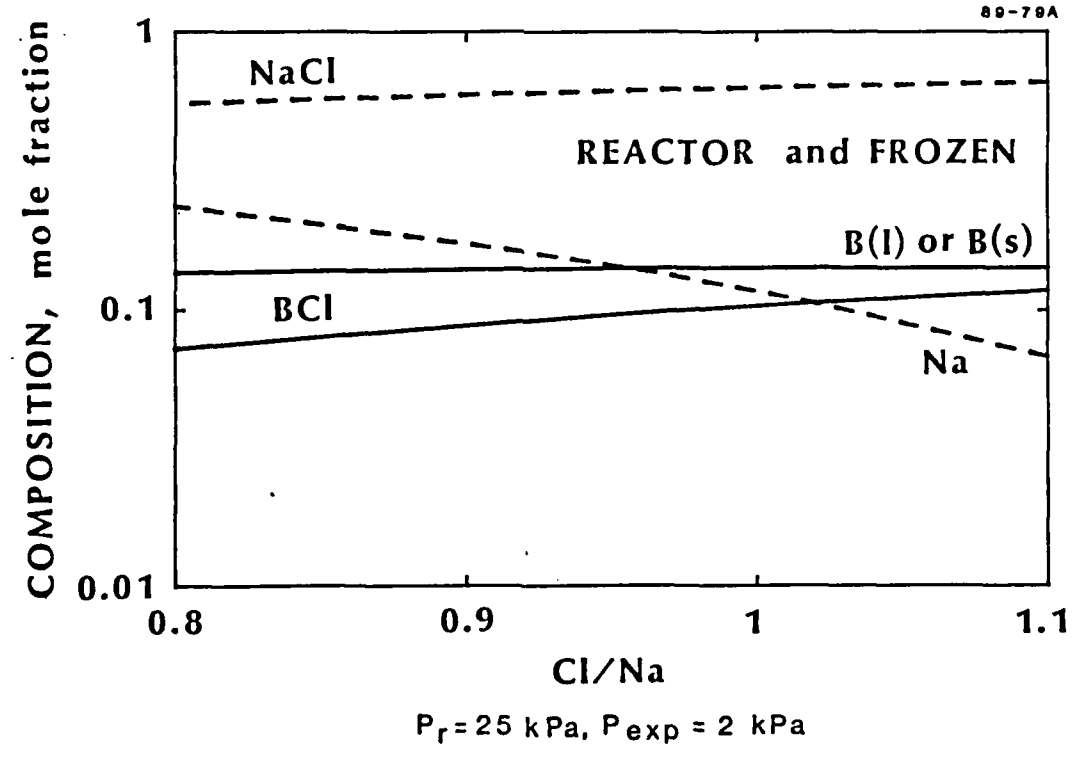

Figure 3. Effect of chlorine sodium ratio on composition in the reactor and for frozen flow

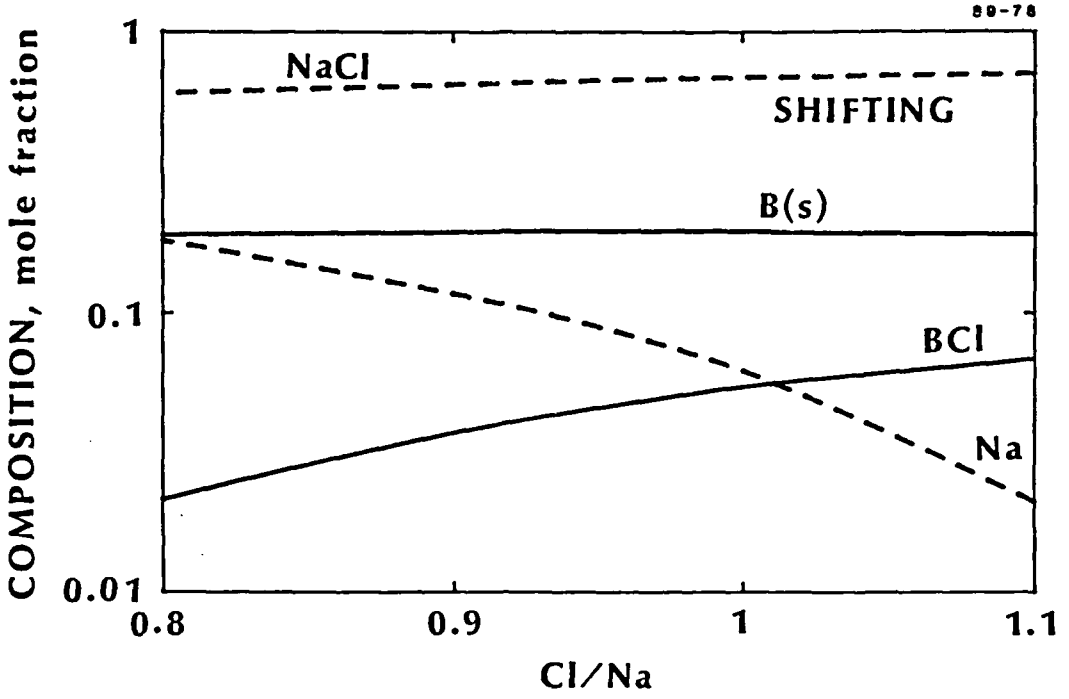

Figure 4. Effect of chlorine sodium ratio on composition for shifting flow

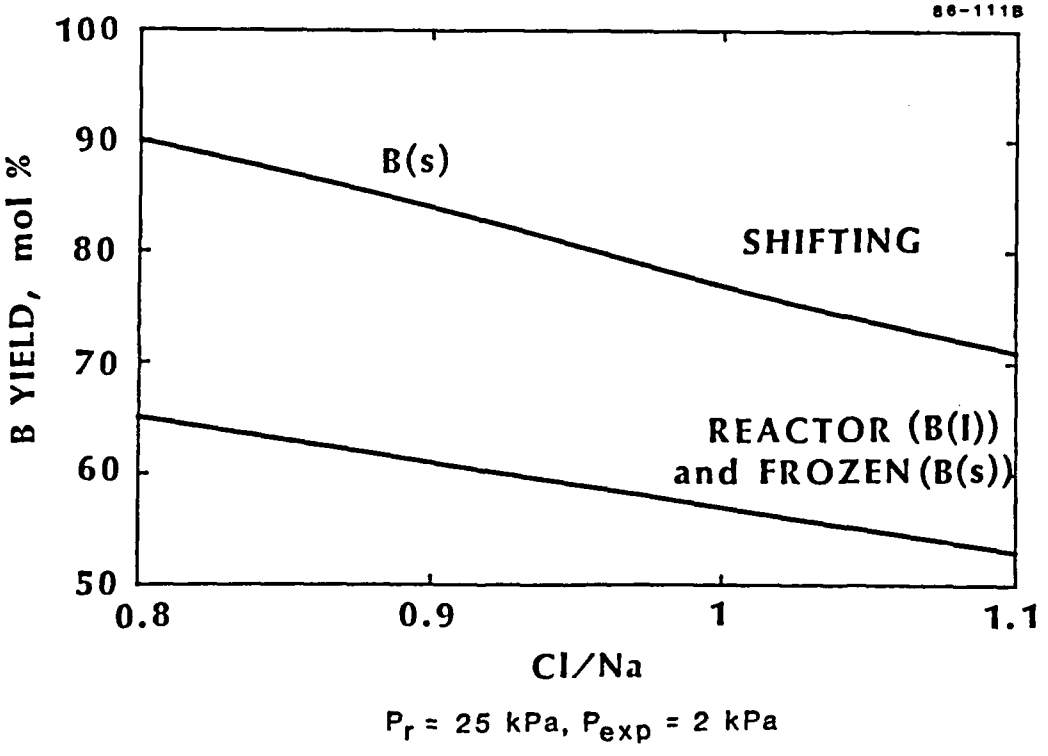

Figure 5. Effect of chlorine sodium ratio on boron yield

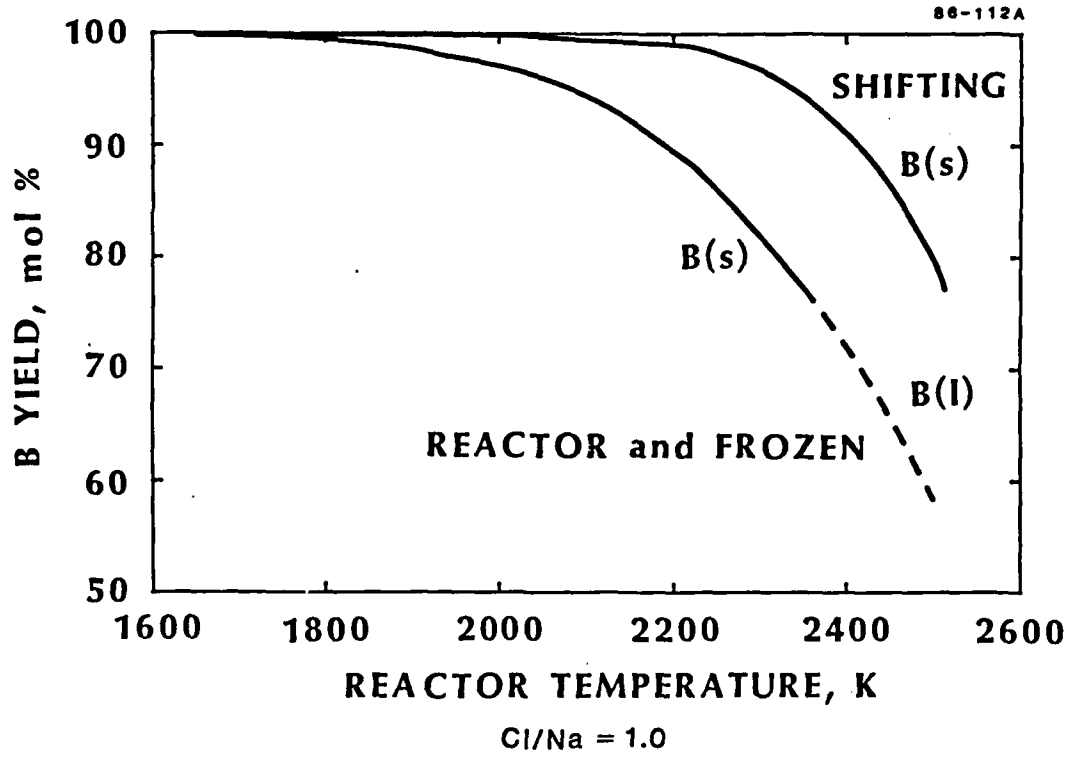

Figure 6. Effect of controlling reactor temperature on boron yield

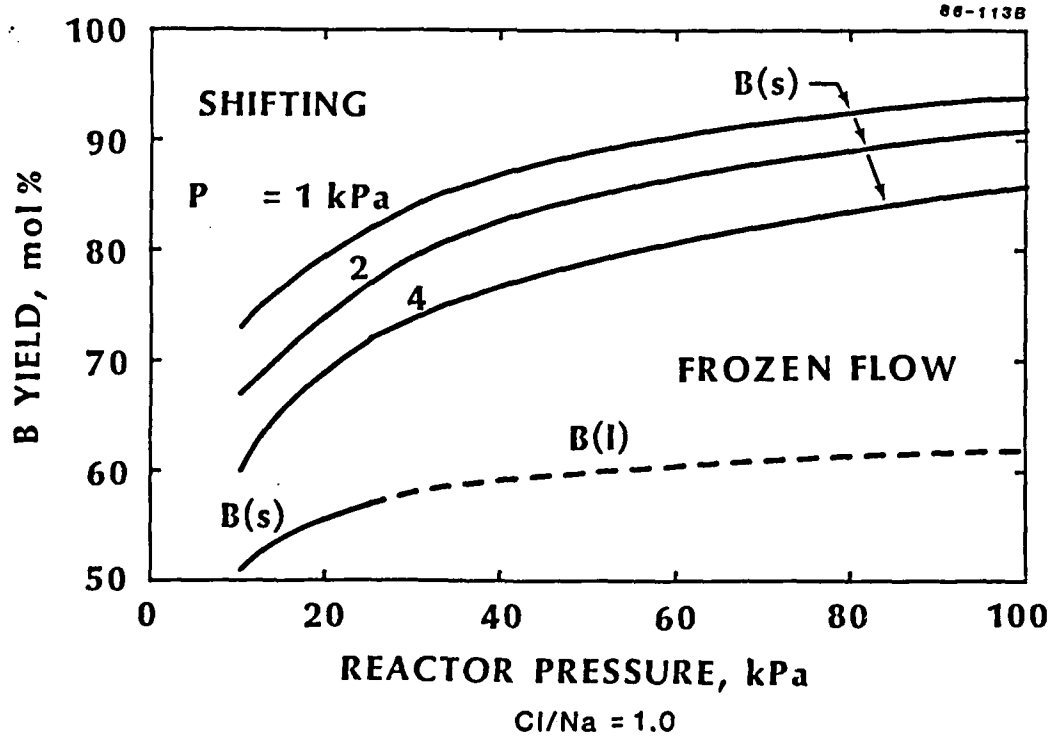

Figure 7. Effect of reactor and downstream pressure on boron yield

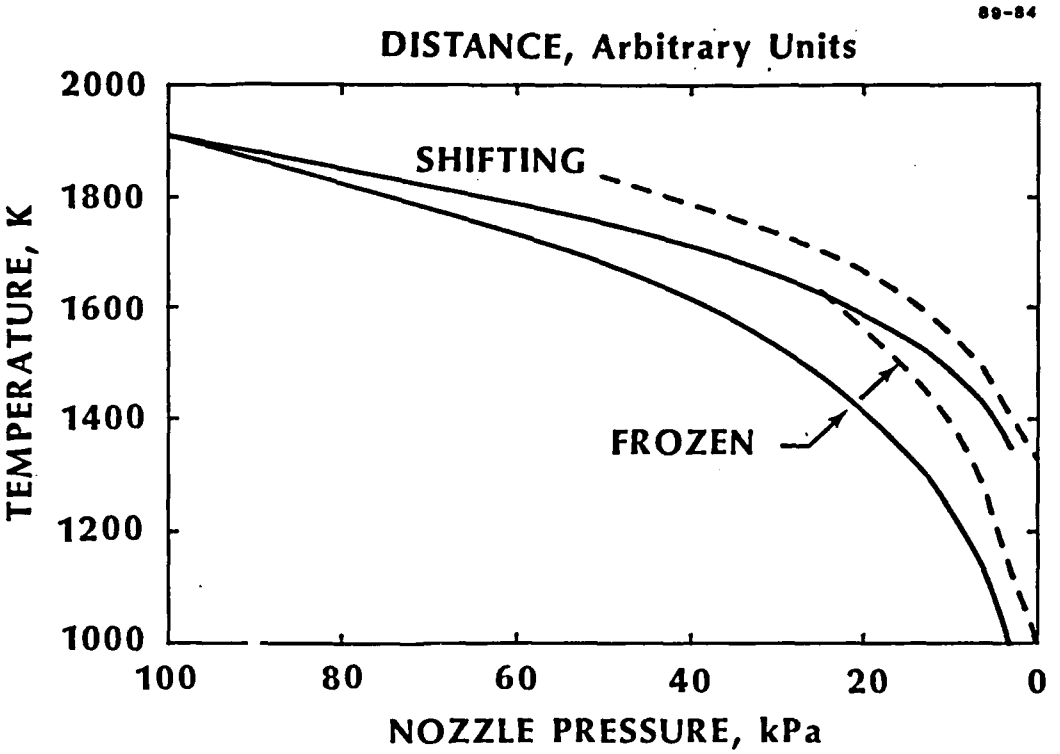

Figure 8. Temperature in nozzle expansion. Without $TiCl_4$ added____; with $TiCl_4$ added in nozzle - - - - -. Input temperature for Na (L) and for BCl_3 (g) = 1100 K; for $TiCl_4$ = 410 K; % $TiCl_4$ to BCl_3 added.

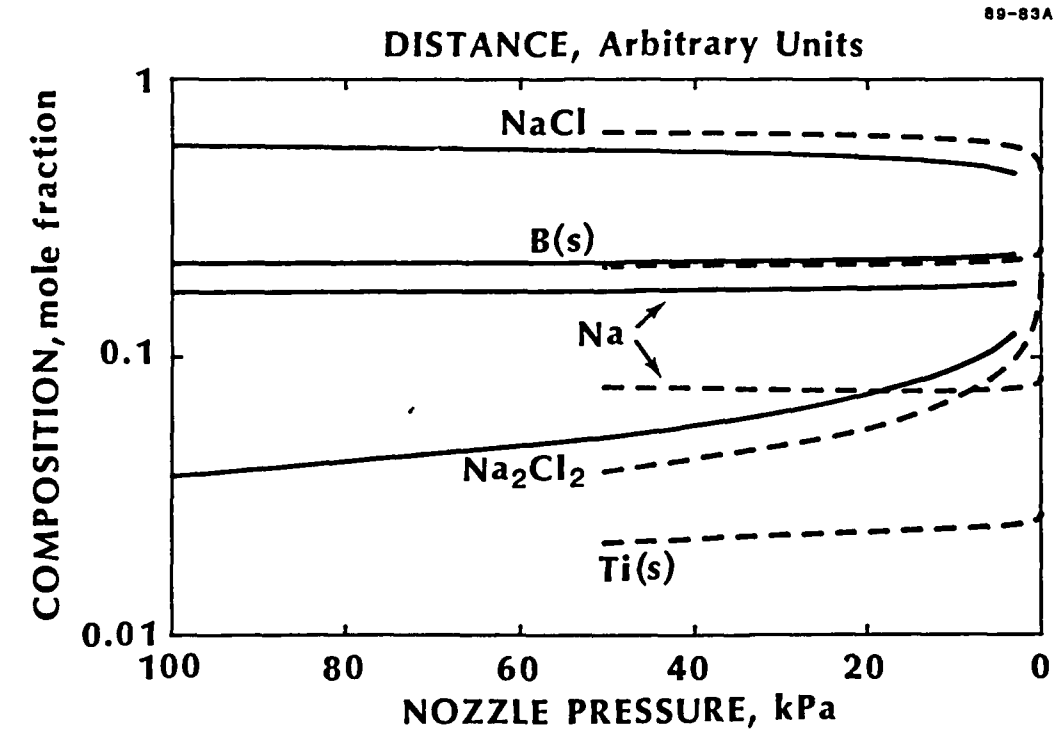

Figure 9. Composition in nozzle expansion. Without $TiCl_4$ added ____; with $TiCl_4$ added in nozzle - - - - -; conditions the same as in Fig. 8.

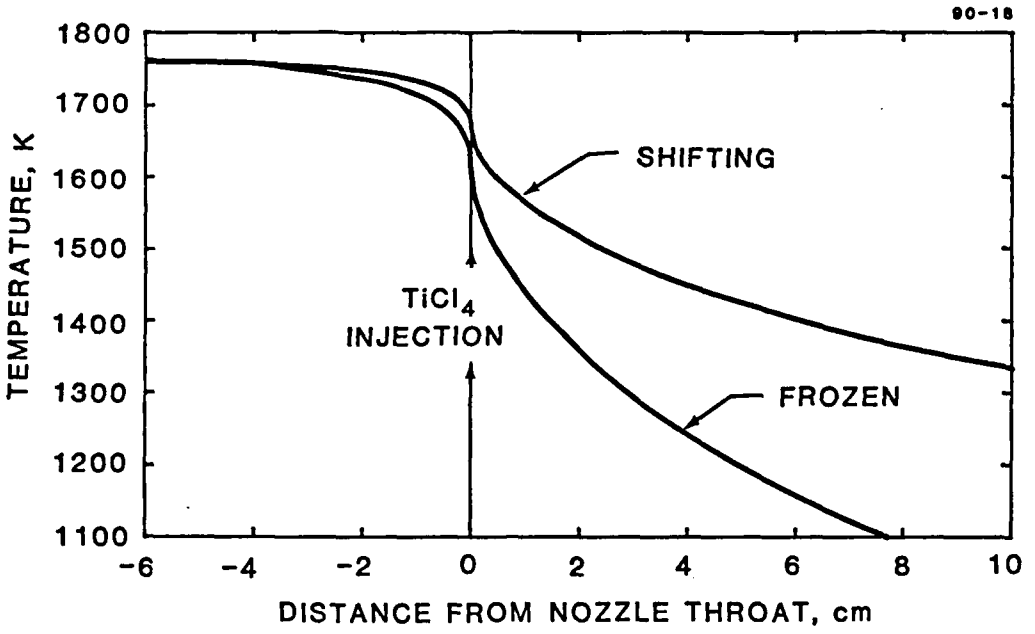

Figure 10. Temperature for shifting and frozen equilibrium. From ISP calculations. From ISP calculations; throat diameter = 0.6 cm; entrance and exit half angles = 2°; reactants (moles): 3.24 Na (L, 700 K) + 1.00 BCl_3 (g, 298 K); 0.226 $TiCl_4$ (g, 410 K) injected in nozzle throat.

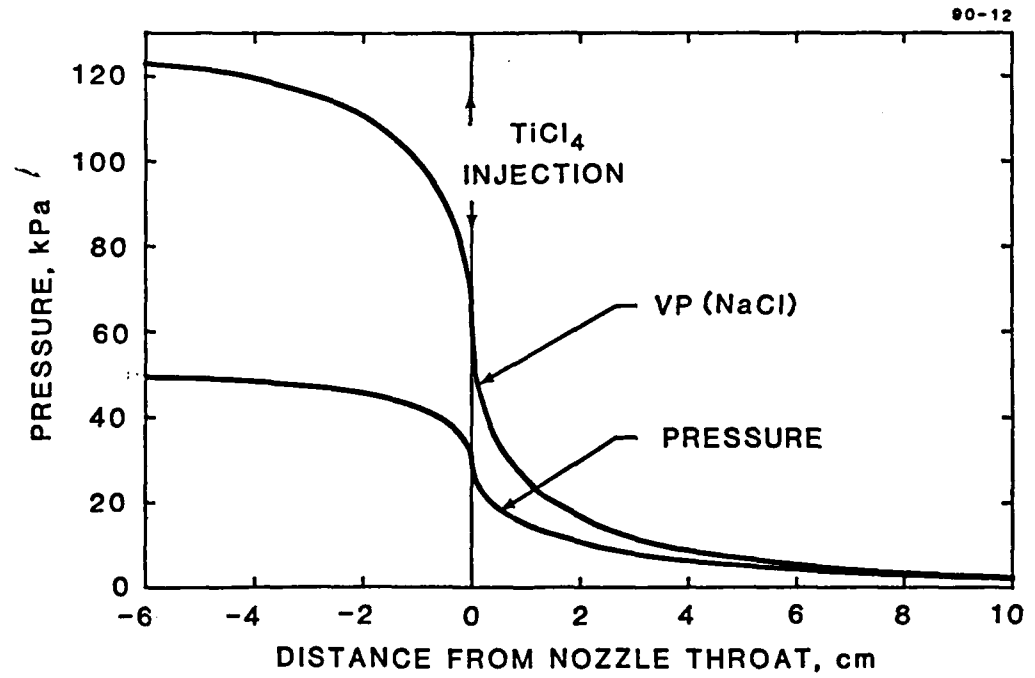

Figure 11. System pressure and vapor pressure of NaCl variation with distance; conditions the same as in Fig. 10. Vapor pressure of NaCl based on shifting equilibrium temperature.

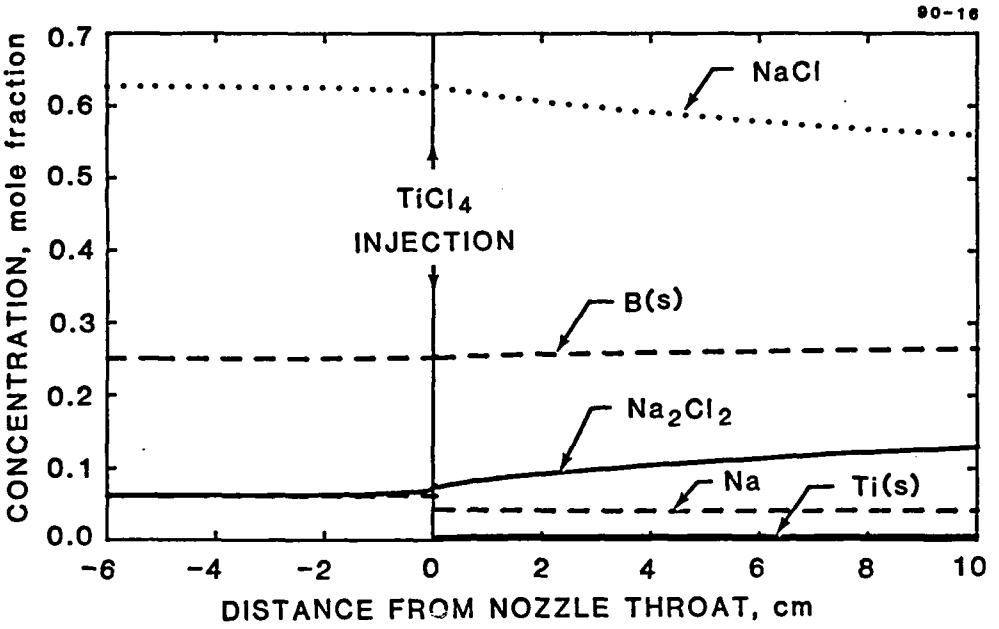

Figure 12. Products for shifting equilibrium flow. From ISP calculations; conditions the same as in Fig. 10.

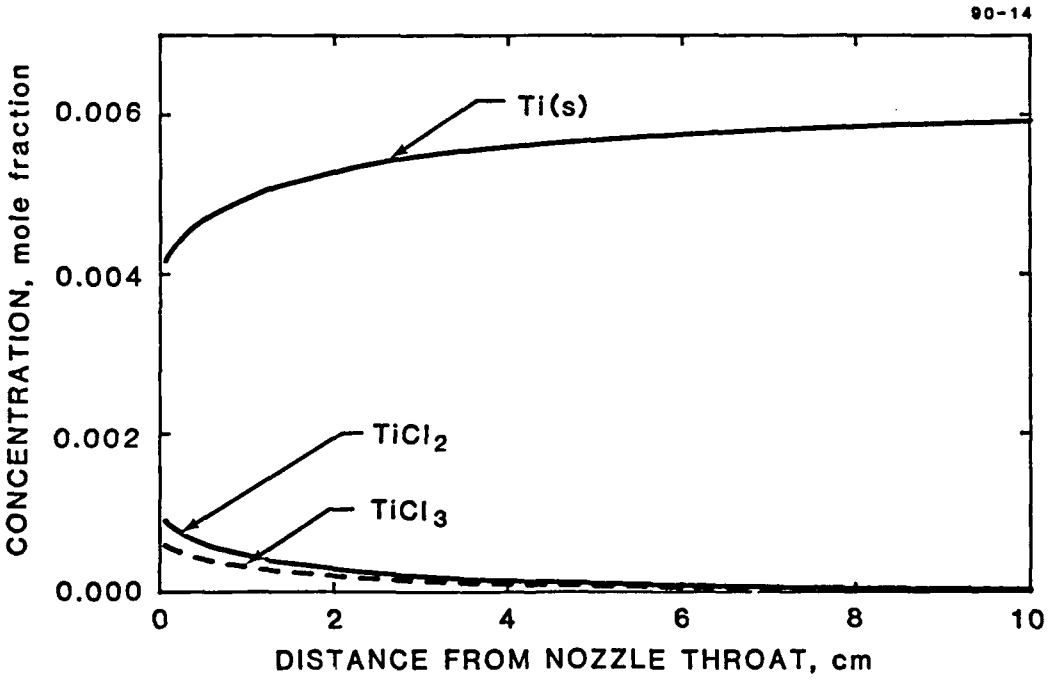

Figure 13. Products for shifting equilibrium flow; conditions the same as in Fig. 10.

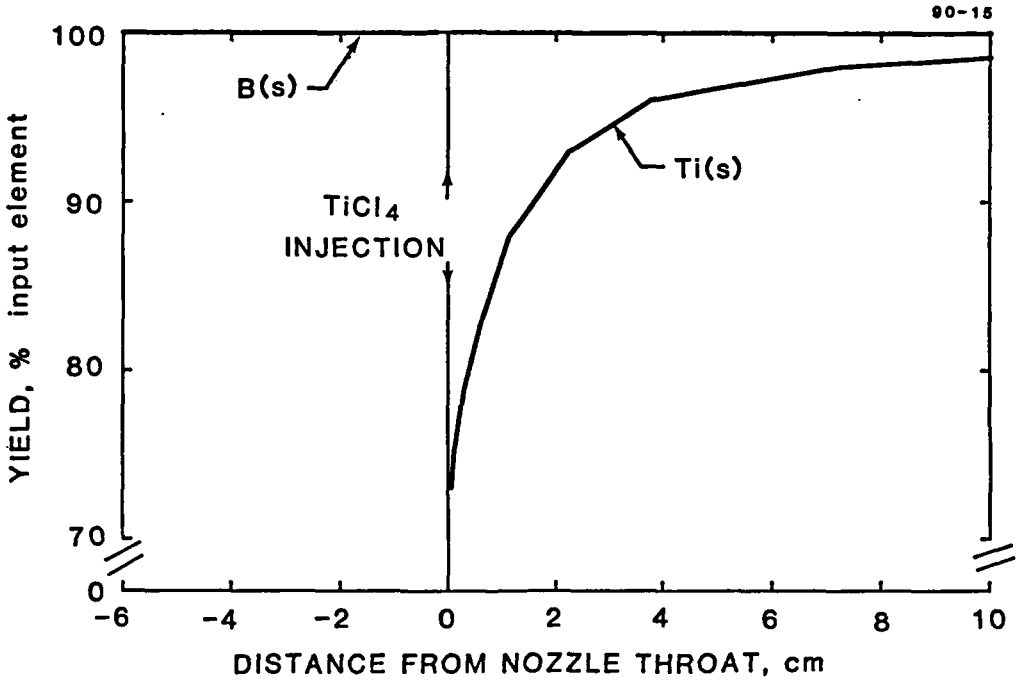

Figure 14. Boron and titanium yields for shifting equilibrium; conditions the same as in Fig. 11.

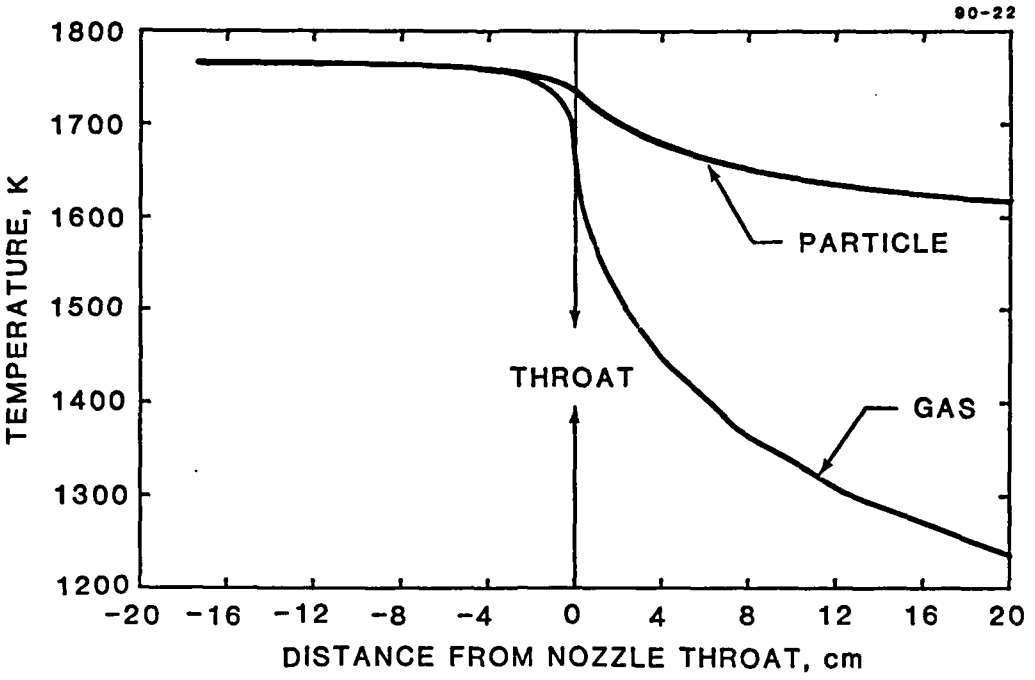

Figure 15. Comparison of particle and gas temperatures without particle growth. 1 μm particle; nozzle throat = 0.6 cm; entrance and exit half angles = 2°; data from Figs. 11 through 12.

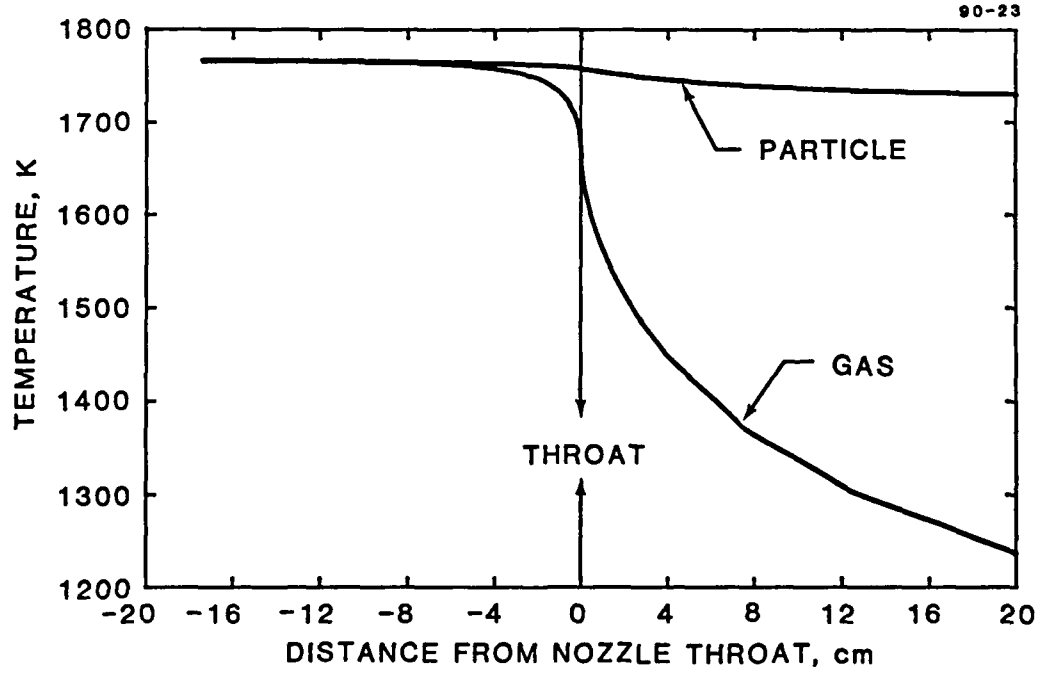

Figure 16. Comparison of particle and gas temperatures without particle growth. 6 μm particle; other conditions the same as in Fig. 15.

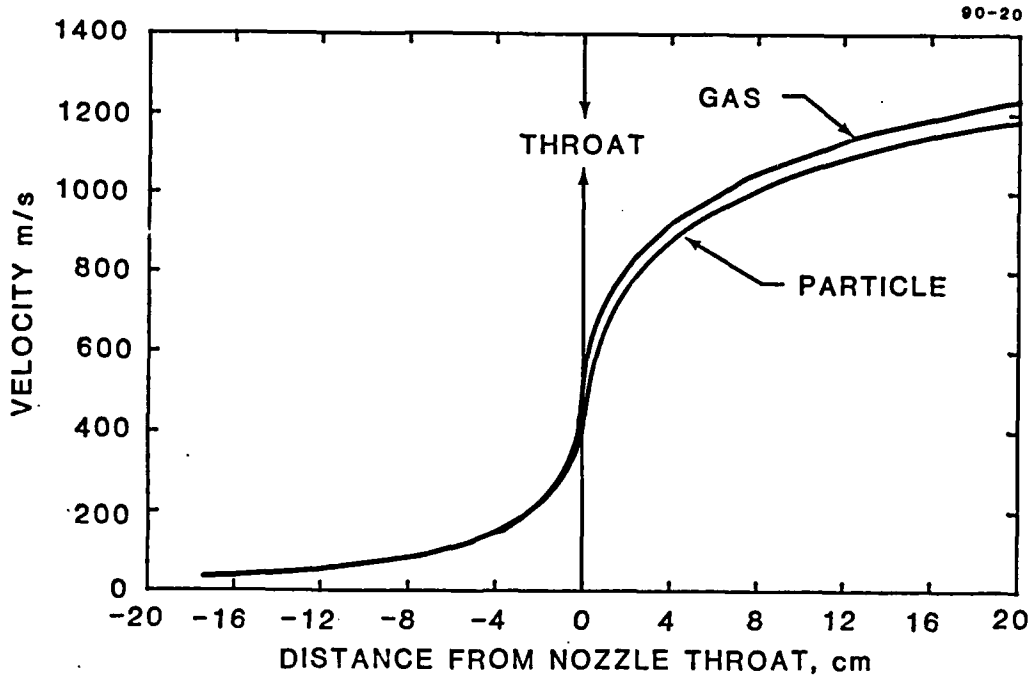

Figure 17. Comparison of particle and gas velocity. 1 μm boron particle; conditions the same as in Fig. 15.

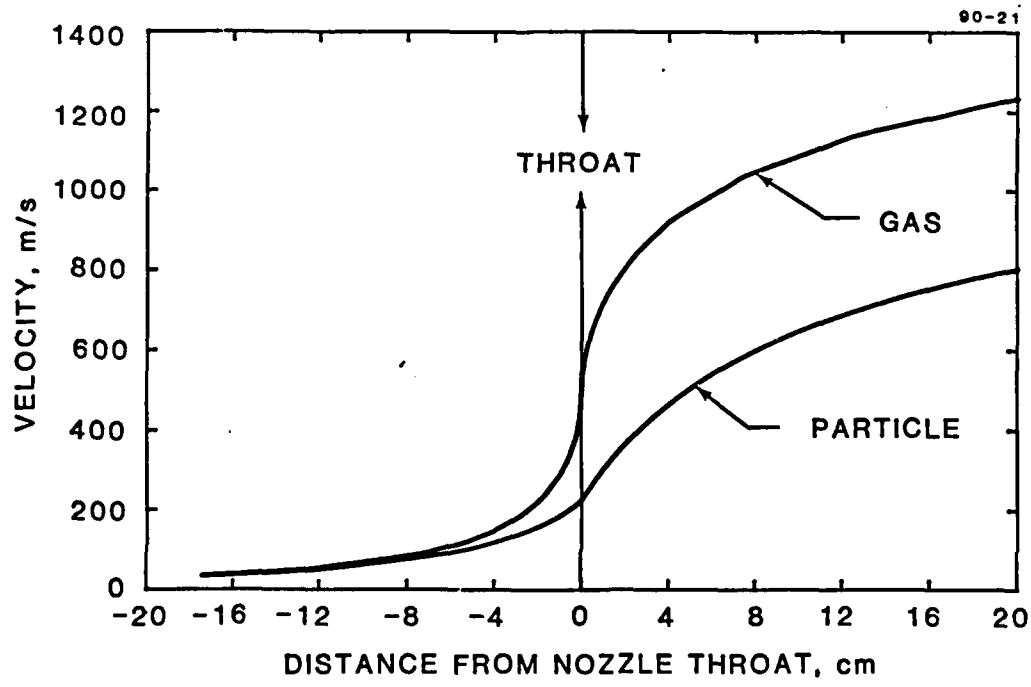

Figure 18. Comparison of particle and gas velocity. 6 μm boron particle.

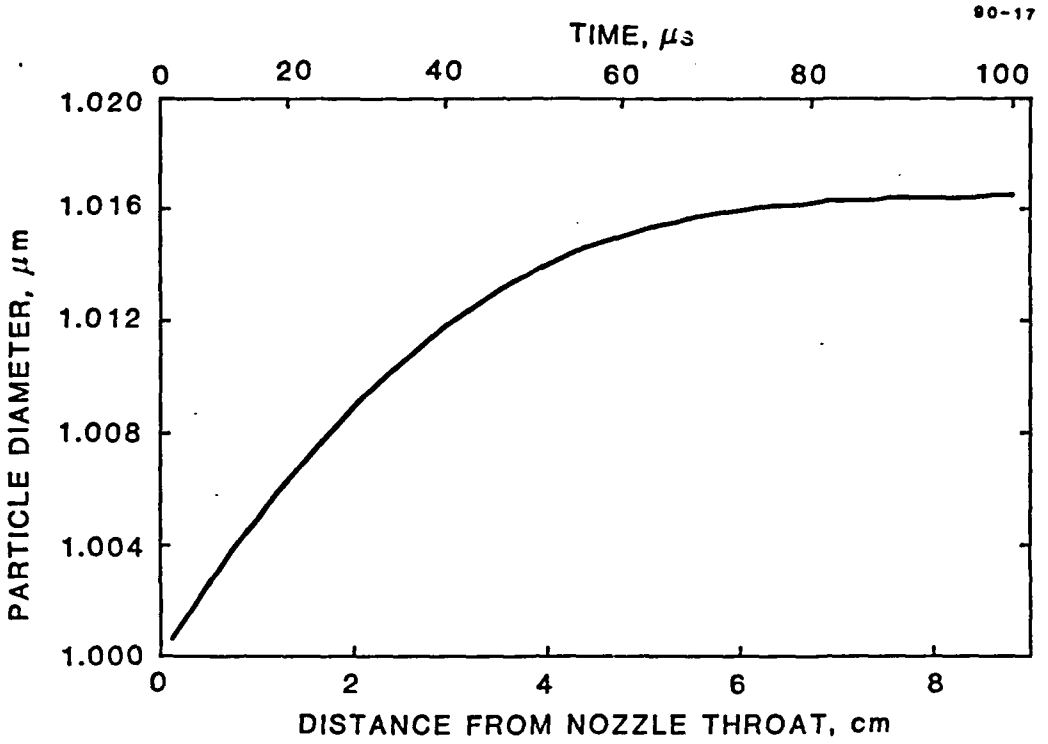

Figure 19. Particle growth. 1 μm initial boron particle; data from Figs. 10, 11, 12, 14, and 17.

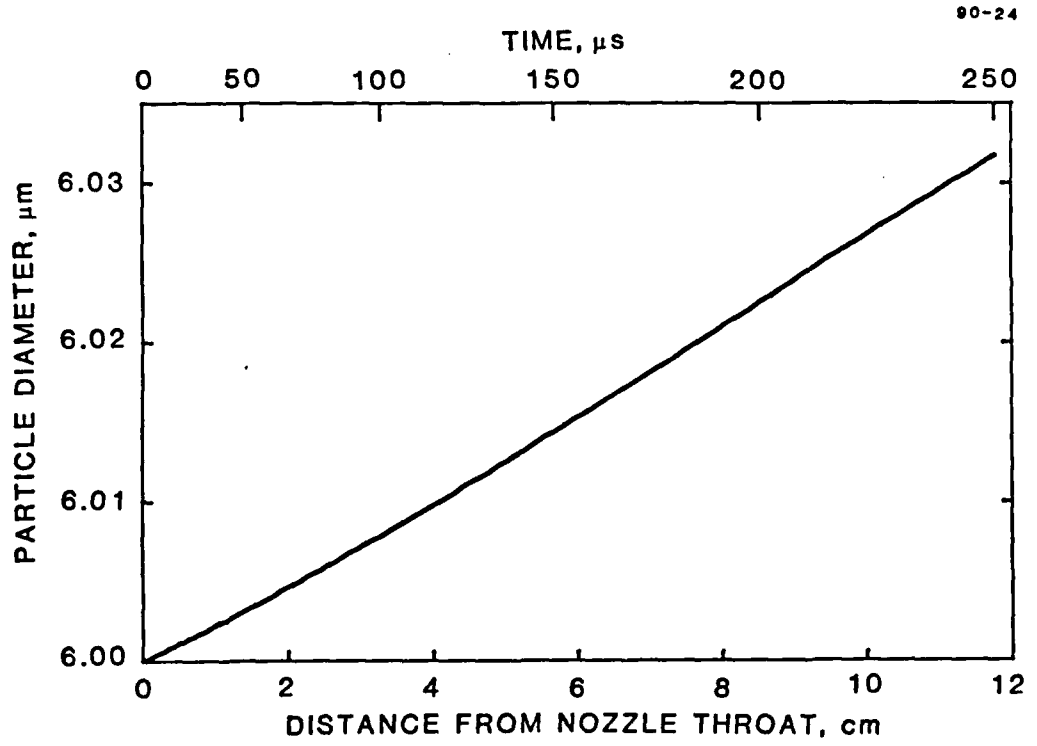

Figure 20. Particle growth. 6 μm initial boron particle; data from Figs. 10, 11, 12, 14, and 18.

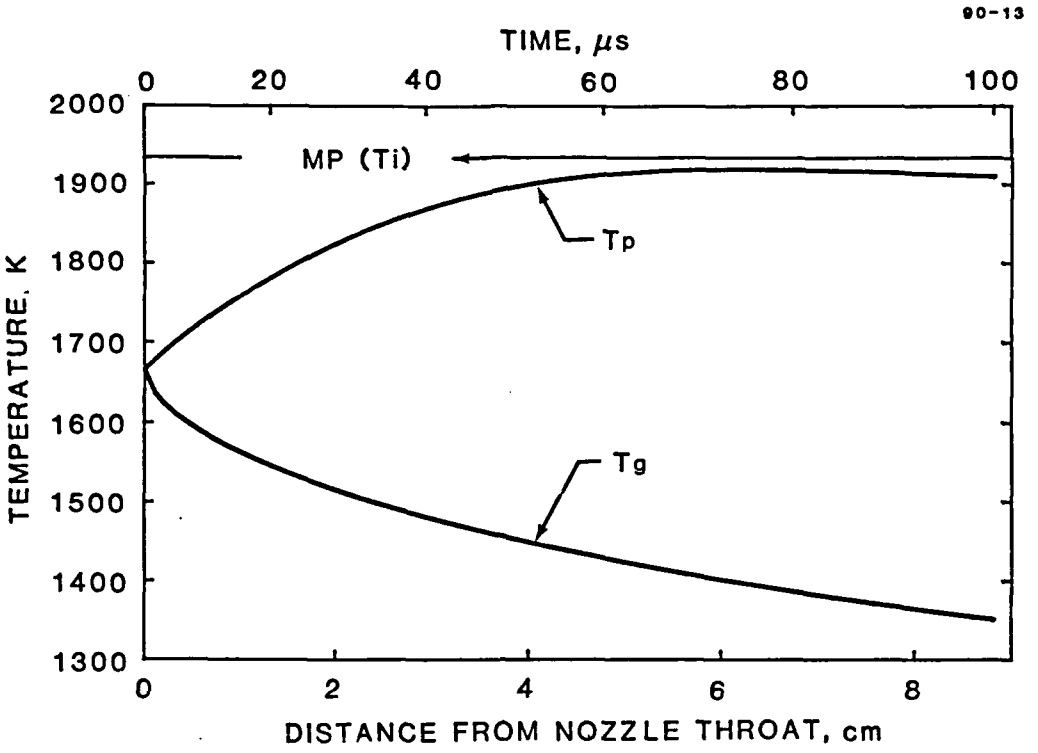

Figure 21. Comparison of particle and gas temperature with particle growth. 1 μm initial boron particle; conditions the same as in Fig. 19.

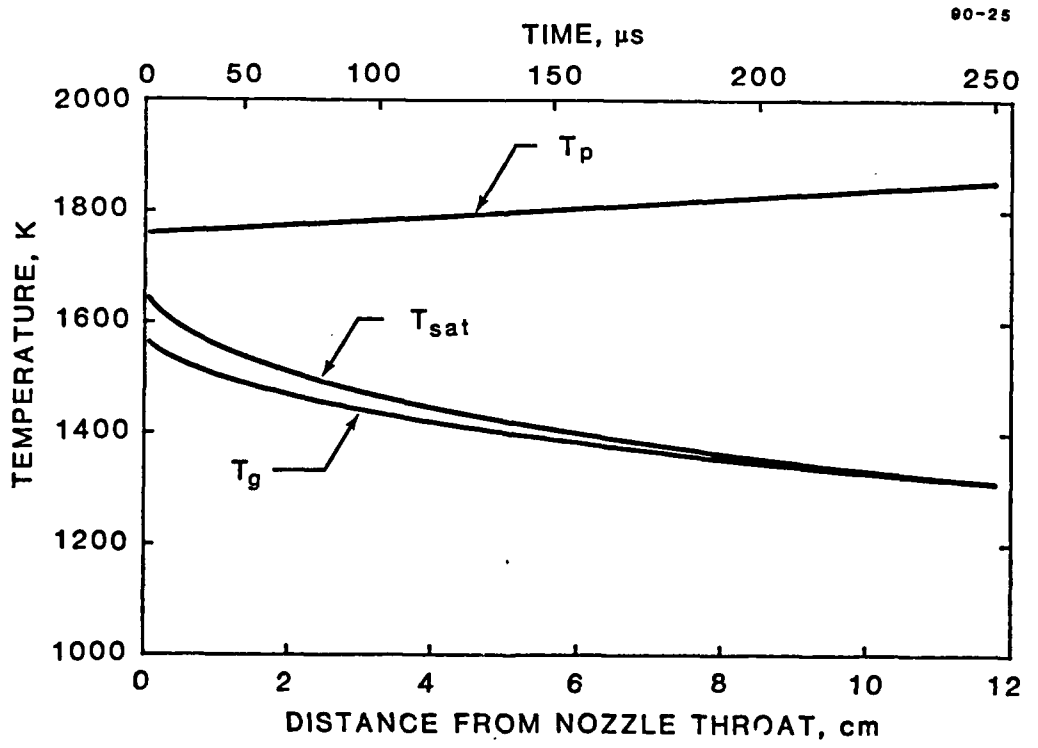

Figure 22. Comparison of particle and gas temperature with particle growth; 6 μm initial boron particle; conditions the same as in Fig. 20.

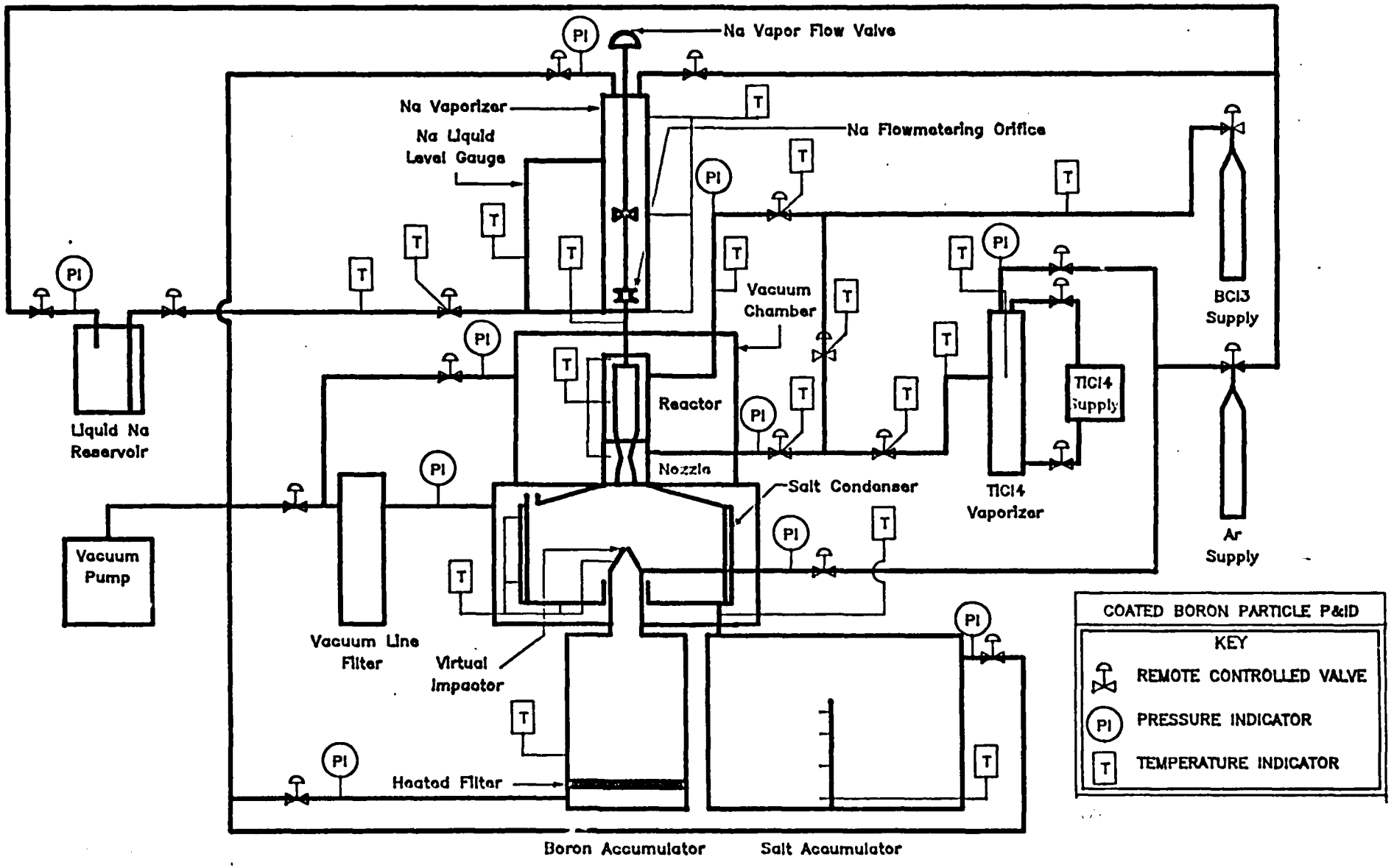

Figure 23. Process and instrumentation diagram for coated boron particle production apparatus

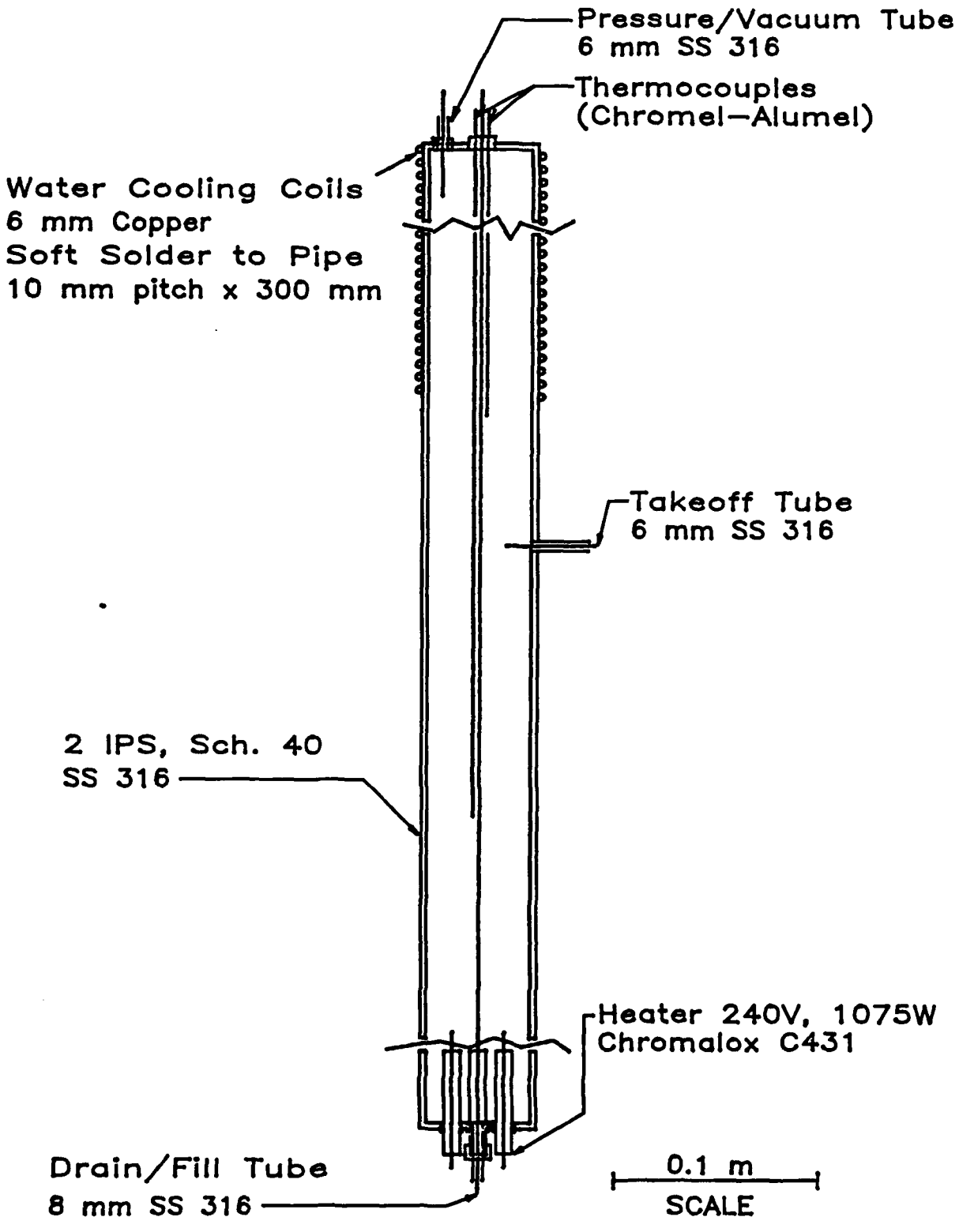

Figure 24. Titanium tetrachloride vaporizer .

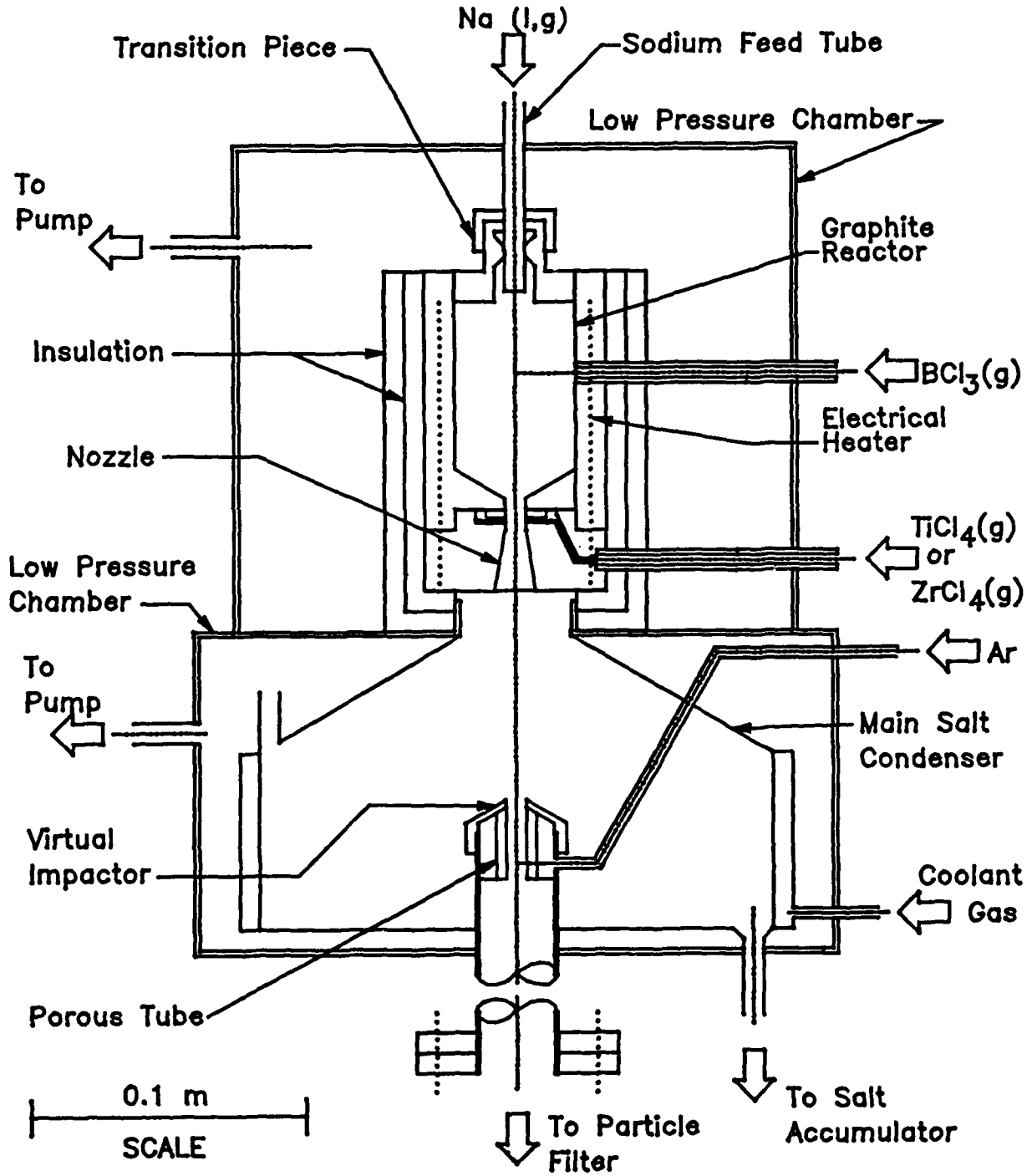

Figure 25. Overall schematic of coated boron powder production apparatus

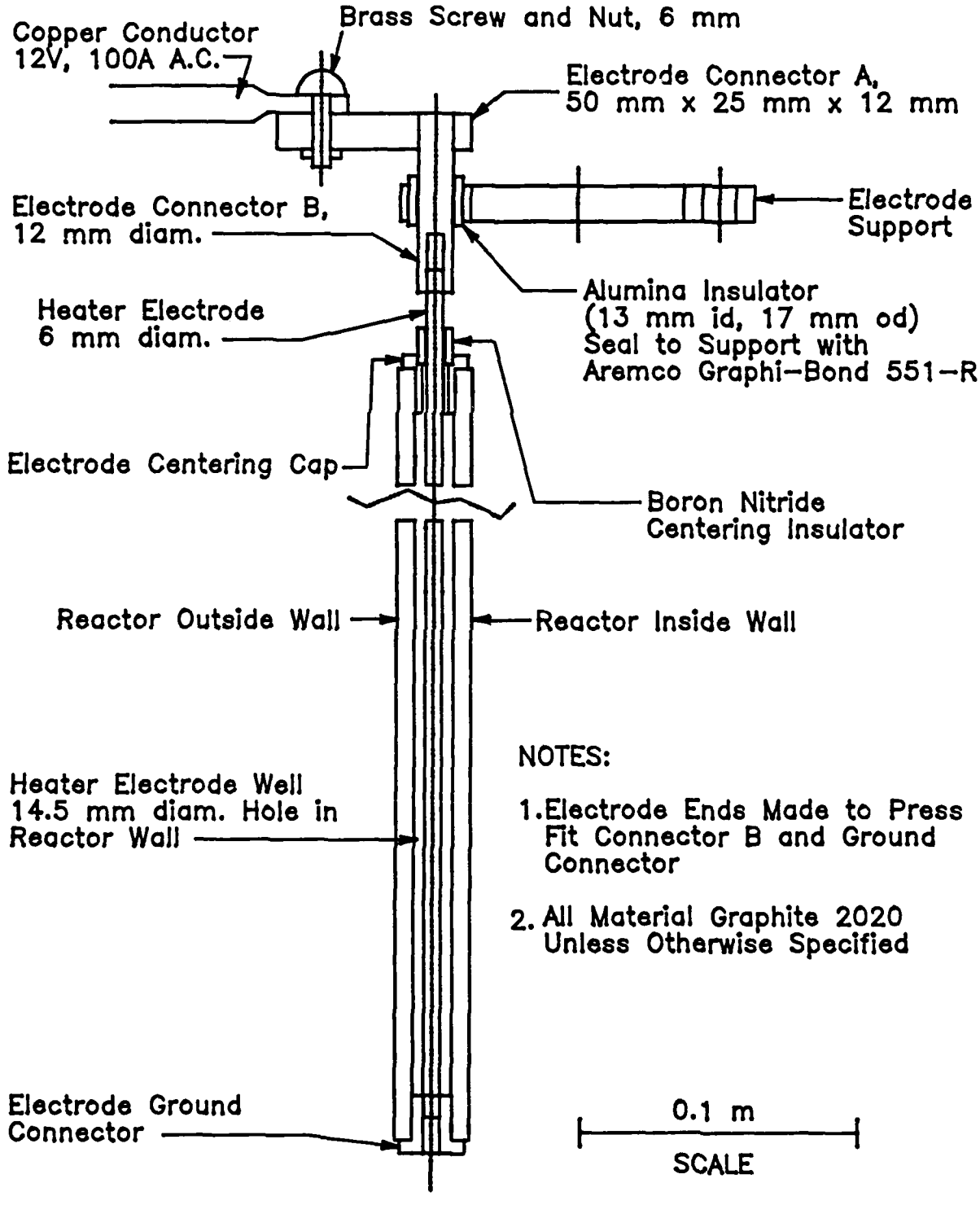

Figure 26. Detail of reactor electrical heater

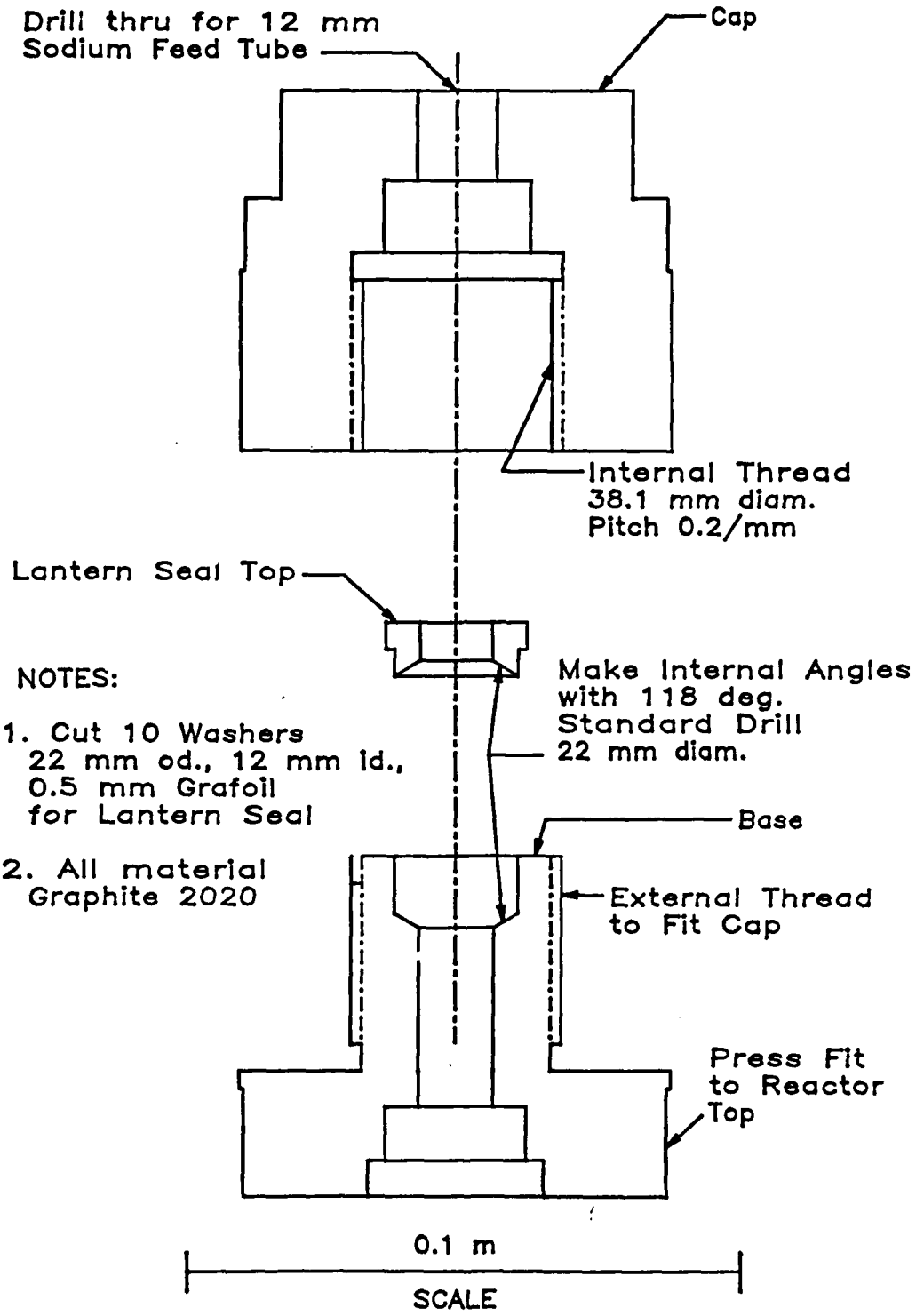

Figure 27. Transition piece

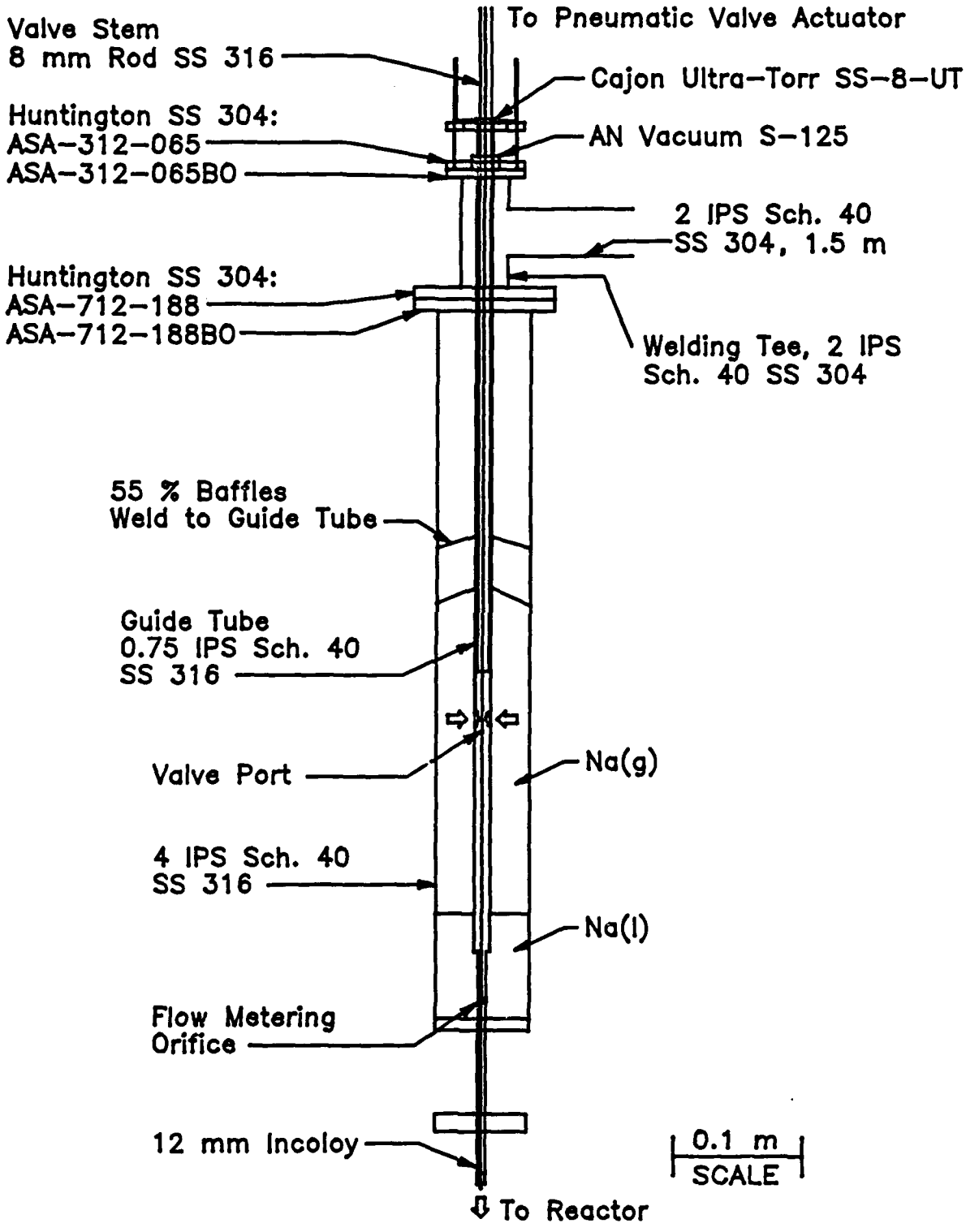

Figure 28. Sodium vaporizer

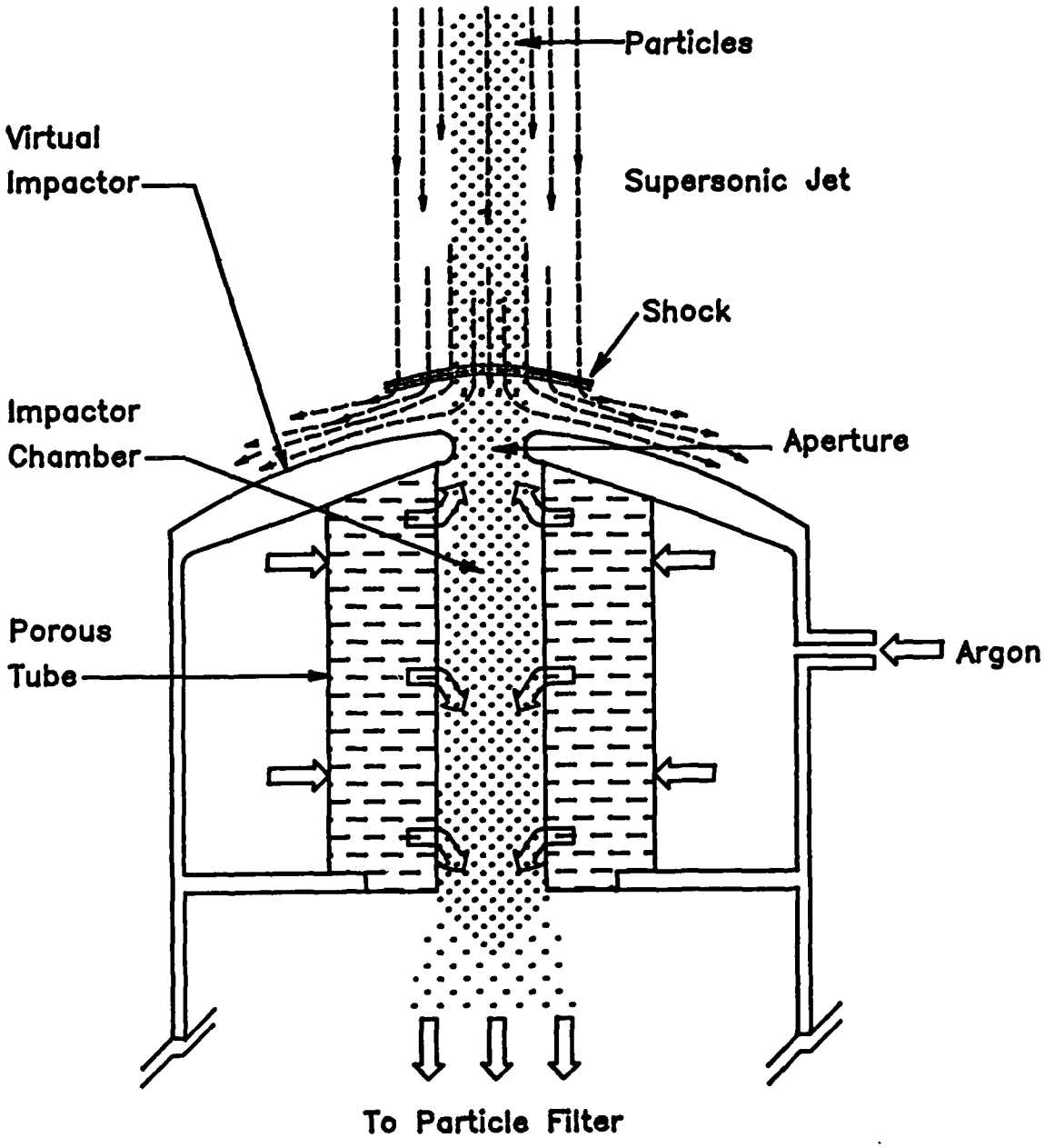

Figure 29. Schematic of supersonic virtual impact collector

Table 1. Preliminary Design Parameters for 300 g/h Coated Boron Powder Reactor

Design unit	P (kPa)	T (K)	Flow rate (mmol/s)	Power (kW)	Material
Na vaporizer[a]	60	1100	32	5	316 ss
BCl_3 feed system[b]	200	300	7.7	1	Monel
$TiCl_4$ feed system[c]	100	410	0.4	0.5	316 ss
Reactor[d]	25	1900	31	12[f]	2020 graphite
Salt condenser[e]	1	1100	32	-6	316 ss
Virtual impactor/boron filter[f,g]	≤ 25	1400	8.9	0.2	2020 graphite
Salt accumulator[h]	1	300	32	-3	316 ss

[a]Use orifice flow meter.
[b]Delivery from cylinder.
[c]Delivery from vaporizer.
[d]Throat 0.6 cm diameter. Volume (chosen same as for silicon reaction) = 0.5 L.
[e]Gas cool to control temperature.
[f]0.75 cm diameter aperture in virtual impactor.
[g]Use ceramic or graphite filter.
[h]Freeze liquid salt.

Table 2. Argon Flows and Filter Diameters for Particle Collection
P_{tot} = 25 kPa, v = 2 cm/s

T (K)	P_{sat} (kPa)	Q_{Ar} (standard L/s)	Q_{tot} (L/s at T,P_{tot})	A_f (m^2)	Diameter (m)
1000	0.01	90.8	1330	66.5	4.60
1100	0.07	12.4	201	10.0	1.79
1200	0.37	2.35	41.8	2.09	0.82
1300	1.50	0.55	11.22	0.558	0.42
1400	4.98	0.14	3.62	0.181	0.24
1500	14.1	0.28	1.37	0.0685	0.15
1560	25.3	0	0.79	0.0397	0.11